Determining Signal-to-Noise Ratio in a Burst Coherent Demodulator

by

Janet Liu

Submitted to the Department of Electrical Engineering and Computer Science
in Partial Fulfillment of the Requirements for the Degrees of

Bachelor of Science in Electrical Engineering and Computer Science
and Master of Engineering in Electrical Engineering and Computer Science

at the Massachusetts Institute of Technology

May 1999
[June 1999]

Author .....
Department of Electrical Engineering and Computer Science
May 28, 1999

Certified by .....
G. David Forney
Thesis Supervisor

Accepted by .....
Arthur C. Smith
Chairman, Department Committee on Graduate Theses

Determining Signal-to-Noise Ratio in a Burst Coherent Demodulator

by

Janet Liu

Submitted to the
Department of Electrical Engineering and Computer Science

May 28, 1999

In Partial Fulfillment of the Requirements for the Degrees of
Bachelor of Science in Electrical Engineering and Computer Science
and Master of Engineering in Electrical Engineering and Computer Science

Abstract

Effective methods of performing diversity selection in wireless systems has been demonstrated to significantly reduce bit error rate. Information about the noise on a channel can allow accurate selection of the best diversity branch. This thesis, based on research conducted at Telcordia Technologies (formerly Bell Communications Research) describes a study of the PACS demodulator. The study was aimed at investigating possible methods of estimating the signal-to-noise (SNR) ratio on a wireless channel. In the interest of maintaining the current system and of taking advantage of the primary features of the PACS system, two quality metrics, based on the phase disturbance of the received signal, were studied to determine their correlation to noise. A description of these metrics and their proposed relationship to noise is provided. Methods to analyze the performance and reliability of the metrics are described, along with a simulation environment for evaluating their performance. Finally, initial results of the analysis is presented, accompanied by a brief evaluation of these results.

Thesis Supervisor: G. David Forney
Title: Adjunct Professor, Electrical Engineering and Computer Science

Acknowledgments

I wish to express my thanks to Rob Ziegler, my supervisor at Telcordia Technologies. Much of the work described in this thesis is due to the simulation efforts of the PACS system that he initiated. He offered me technical guidance and support and often went beyond the call of duty to assist me and to give me a positive experience during my time away from campus.

I would also like to thank Telcordia Technologies and the MIT VI-A Program for sponsoring this thesis and for providing me with an opportunity to do research in a corporate environment. I will always consider it a valuable part of my MIT education. Thank you to all the faculty who have taught me many new and exciting things in my five years here. They have also provided me with an irreplaceable education. Final thanks to my on-campus supervisor, Dr. G. David Forney, particularly for his editorial contributions to Section 2.2 of my thesis document.

I would like to thank my family for all they have done for me these years. My journey through MIT is as much their accomplishment as it is mine. Thank you for loving me and supporting me through the entire experience. I could not have done anything without them.

I would like to thank my friends, my church, and my fellowship who have been incredibly supportive and encouraging throughout this whole process. They have been my family here, and I appreciate the loving kindness they have never failed to show me. Special thanks for their many prayers and encouragements. It made all the difference.

To my family and friends: Your unconditional love has humbled and reminded me to focus on what is important. If I were to choose the one thing I learned the most from this experience, it would be how precious God's people are and how much I need everyone God has put into my life.

Lastly, and most importantly, I would like to thank my Father in heaven, and my Lord and Savior, Jesus Christ for His abundant grace and love. You give me life in full, and all blessings in abundance. I owe all of who I am and what I have to You. I pray this experience has been to Your glory.

Contents

List of Figures

Chapter 1

Introduction

In the past decade, the demand for commercial mobile communications has risen dramatically. Implicit in the demand for wireless communication is the need for highly reliable and affordable service, equally accessible from a variety of environments: urban, suburban, and rural; indoor and outdoor. In response to these demands, the telecommunications industry has developed several standards designed to specify delivery of these services to the various types of regions.

Two types of cellular service have been developed to meet the needs of an increasingly mobile society: high-tier and low-tier cellular service. High-tier cellular is characterized by high-power transmitters and macro-cell coverage and is designed for subscribers moving at vehicular speeds. Low-tier systems feature low-power transmitters and micro-cell coverage and provide the complementary service to subscribers moving at pedestrian speeds.

There are several high-tier and low-tier standards in place globally. GSM, TDMA, and CDMA are the common high-tier standards in Europe and North America. They have met with considerable success in their respective regions of operation. Low-tier standards have been less widely deployed in the U.S., although the Personal Handyphone System (PHS) has been well accepted in Japan. Two other low-tier standards, Digital European Cordless Telecommunications (DECT) and Cordless Telephone second generation (CT2), have formed the basis for private branch exchange (PBX) products [1].

One final standard, developed in the U.S., is Personal Access Communications System (PACS). A significant portion of the PACS development work was done at Telcordia Technologies (formerly Bell Communications Research), and some unique technology has

emerged relating to this standard. Currently, there is extensive work being done to develop a PACS handset, which boasts a low-overhead burst coherent demodulator and a design that takes advantage of many of the features of the PACS standard. Development work in this area is continuing to expand to include not only the hand-held device, but also a full-service wireless local loop and a third-generation wireless system with wireless LANs.

1.1 Personal Access Communications System (PACS)

PACS is an ANSI standard for 1900 MHz low-tier Personal Communications Systems (PCS) service. It is characterized by micro-cell coverage, low transmit power, and low complexity, and is ideal for neighborhood applications, such as indoor wireless, wireless local loop, and pedestrian venues. It offers several advantages over macro-cell systems. For instance, PACS equipment is simpler and less costly and operates with a lower delay, and yet is more robust than indoor systems. Moreover, PACS has demonstrated satisfactory operability under high-speed vehicular mobility conditions and is well-suited to deliver high capacity, superior voice quality and ISDN data services. Therefore, PACS is a viable solution to providing high user density in both indoor and outdoor environments [2].

PACS technology is being developed because it can be combined ideally with the traditional high-tier services, already in widespread use, for complete wireless service. PACS is able to provide virtually land-line quality service using radio ports that are simple and low-cost. With such an affordable and reliable low-tier standard, wireless technology could easily become a viable alternative to traditional land-line phones. In particular, countries with under-developed telephone switching systems could avoid costly installations of miles of wires and switching centers.

Given this motivation for developing PACS technology, providing the best quality at the fastest rate is a major goal.

1.2 Diversity Selection

In wireless environments, diversity selection becomes an important issue. The ability to increase the quality of a received signal is essential. There are many techniques that can be used to achieve this goal. Increasing the power of the transmitted signal, and thereby increasing the signal-to-noise ratio (SNR), is one approach. In a typical additive white

Gaussian noise channel, this method is quite effective in its ability to decrease the bit error rate of the signal. However, practical constraints prevent wireless hand-held systems from transmitting signals with unlimited power. Therefore, additional methods effective in reducing error rate must be employed in combination with higher transmit power. For instance, in a typical multipath fading channel environment, diversity selection has been shown to improve SNR more efficiently than higher transmit power or additional bandwidth [1].

In particular, branch diversity selection is often employed to mitigate the effects of Rayleigh fading. This type of branch selection can be made on the basis of the best signal-to-noise ratio. Therefore, being able to accurately estimate the SNR on a given channel is central to this selection method and to the quality of the received signal [3]. Developing effective methods of diversity selection is crucial to the performance of a wireless communications system.

We are therefore motivated to study methods that can improve diversity selection. We describe an efficient method that is easily incorporated into the overall system. Minimizing additional hardware and computational complexity are major constraints on the overall goal of improving diversity selection. However, the PACS demodulation algorithm offers several key features which can be exploited and used to estimate the SNR on a given channel and ultimately to aid in diversity selection. This thesis studies the demodulation algorithm, its unique features, and the design of the hardware system and presents results that may offer insight into developing future methods of diversity selection based on symbol timing.

The following chapters will discuss various aspects of the project and the methods investigated. Chapter 2 describes the PACS system and establishes the background for the research described in the following chapters. Chapter 3 states the objective of the thesis and provides a theoretical discussion of the principles underlying our study. Chapter 4 is an overview of the design of the models used in the simulations and experiments. Chapter 5 describes the simulation and analysis systems applied to the data in order to provide a measure of the metrics' ability to accurately estimate SNR and states the results from these simulations. Finally, Chapter 6 summarizes the overall conclusions from this study, including recommendations for future work, and gives the author's perspective on further research and development in this area.

Chapter 2

Background: System Overview

This chapter presents an overview of the pertinent elements of the PACS system design. A block diagram of the stages of the demodulation process is shown in Figure 2-1. The

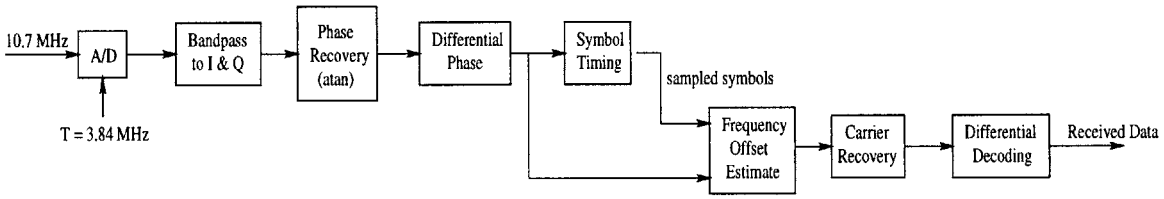

Figure 2-1: Block Diagram of PACS Demodulator

initial portion of the demodulation, in which the baseband signal is converted into phase information, also plays a crucial role and will be discussed in detail. Following this bandpass-to-phase portion, the demodulator circuit is then divided into several stages: symbol timing and frequency estimation, coherent carrier recovery, and differential decoding.

One of the primary motivations for this study is to improve the performance of current diversity selection techniques. It is desirable to be able to choose a diversity branch early in the demodulation process, and consequently, the majority of the research will focus on the bandpass-to-phase portion of the circuit, which precedes the decoding of the signal. Specifically, the symbol timing and frequency estimation portion of the demodulation circuit will be the primary focus of this study because many of the intermediate values computed to perform symbol timing contain information that is correlated with the noise and interference in the signal and will therefore consider many of the same noise issues relevant to diversity selection.

2.1 Modulation

There are a number of issues involved in choosing a modulation technique for wireless communication. For instance, some of the considerations include intersymbol interference, spectral efficiency, power spectral efficiency, and out of band power. Quadrature phase shift keying (QPSK) modulation is often preferred for its greater spectral efficiency. Furthermore, phase modulation, in general, provides an advantage since amplitude information is more vulnerable to the fading environments typical of wireless communication systems. The PACS system uses $\frac{\pi}{4}$-shifted QPSK.

QPSK is a form of quadrature amplitude modulation (QAM), where the transmitted symbol at time i is $z_i = e^{j\theta_i}$, where the phase variable θ_i takes on one of four equally-spaced phase values. In $\pi/4$-shifted QPSK, the set of possible phase values shifts by $\pi/4$ at every time i. In this manner, there is a guaranteed phase change between adjacent symbols, and the differential phase

$$\Delta\phi_i = \theta_i - \theta_{i-1}$$

is always equal to an odd multiple of $\pi/4$. In fact, this characteristic will be a significant feature in the symbol timing circuit design and also in the method being described in this thesis. Figure 2-2 illustrates the phase constellations of this particular modulation scheme and the possible phase transitions between two adjacent symbols.

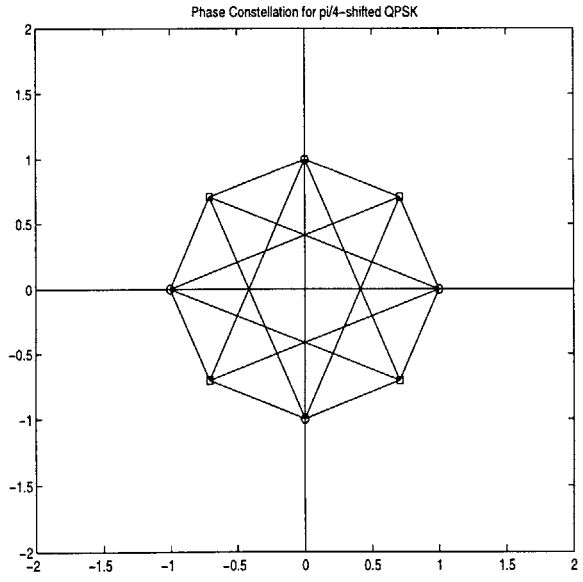

Figure 2-2: Phase Constellation for $\frac{\pi}{4}$-shifted QPSK

Furthermore, a $\frac{\pi}{4}$-shifted QPSK modulation scheme offers several other design advantages for wireless systems. For instance, it provides the spectral efficiency of QPSK systems but with reduced amplitude fluctuations. Furthermore, not only does this method guarantee phase changes with every symbol, it also avoids phase changes through the complex origin. Zero-crossings require power amplifiers to maintain linearity across a wide-amplitude range [5].

2.2 Square-Root-of-Raised-Cosine Nyquist Filtering

The data stream generated by the modulation must then be conveyed as the amplitude values of a signaling pulse shape, $g(t)$. The design of the pulse shaping signal is determined by several constraints placed on its performance. The pulse shape should both minimize intersymbol interference (ISI) and also make the most efficient use of the spectrum of a band-limited channel. The PACS systems uses a square-root-of-raised-cosine transmit and receive filters, or pulse shaping signals. It has been shown in [6] that a square-root of raised-cosine pulse-shaping filter is the optimal choice for both the transmit and receive filters for minimal ISI and maximum SNR.

Using this method, the symbol sequence $\{z_i\}$ is modulated by quadrature amplitude modulation (QAM) using a square-root-of-raised-cosine transmit filter with impulse response $g(t)$. The transmit signal is

$$s(t) = \Re\{x(t)e^{j\omega t}\} = x_r(t)\cos(\omega t) - x_i(t)\sin(\omega t),$$

where $x_r(t)$ and $x_i(t)$ are the real and imaginary parts of the complex signal

$$x(t) = \sum_i z_i g(t - iT),$$

$\{z_i\}$ is the complex $\pi/4$-shifted QPSK symbol sequence, $g(t)$ is a real square-root-of-raised-cosine impulse response, T is the symbol interval in sec, and ω is the carrier frequency in radians/sec.

For this study we will use a simple ideal additive white Gaussian noise (AWGN) channel

model. The received signal is simply

$$r(t) = s(t) + n(t),$$

where $n(t)$ is AWGN with one-sided power spectral density N_0.

The receiver is a QAM demodulator using a matched square-root-of-raised-cosine receive filter $g(t)$. After demodulation to baseband, the received signal is the complex signal

$$r'(t) = e^{j\theta_o} x(t) + n'(t),$$

where $n'(t)$ is still AWGN with one-sided power spectral density N_0, and θ_o is a phase offset due to incorrect phase and/or frequency of the demodulating carrier. (It turns out that in a differential-phase-modulated system the phase offset may be ignored.) The baseband signal is then filtered in the receive filter and sampled every T sec.

The sample sequence r_i is given by

$$r_i = \int r'(t) g(iT - t)\, dt.$$

Because $g(t)$ is real and even, this is equivalent to

$$r_i = \int r'(t) g(t - iT)\, dt;$$

Note that because a square-root-of-raised-cosine filter is square-root-of-Nyquist, the T-shifted filter responses $\{g(t - iT)\}$ are orthonormal; therefore

$$r_i = e^{j\theta_o} x_i + n_i,$$

where x_i is the transmitted symbol and $\{n_i\}$ is an i.i.d. Gaussian sequence with variance $\sigma^2 = N_0/2$ per dimension.

In other words, there is no intersymbol interference and the phase offset θ_o comes through coherently.

2.3 Bandpass-to-Phase

The bandpass-to-phase portion of the circuit will be emphasized because the majority of the methods developed in this study will take place in this particular sub-system. From Figure 2-1, this is the portion that receives the transmitted signal as its input and precedes the decoding of the signal. A more detailed block diagram of the bandpass-to-phase portion of the circuit is provided in Figure 2-3.

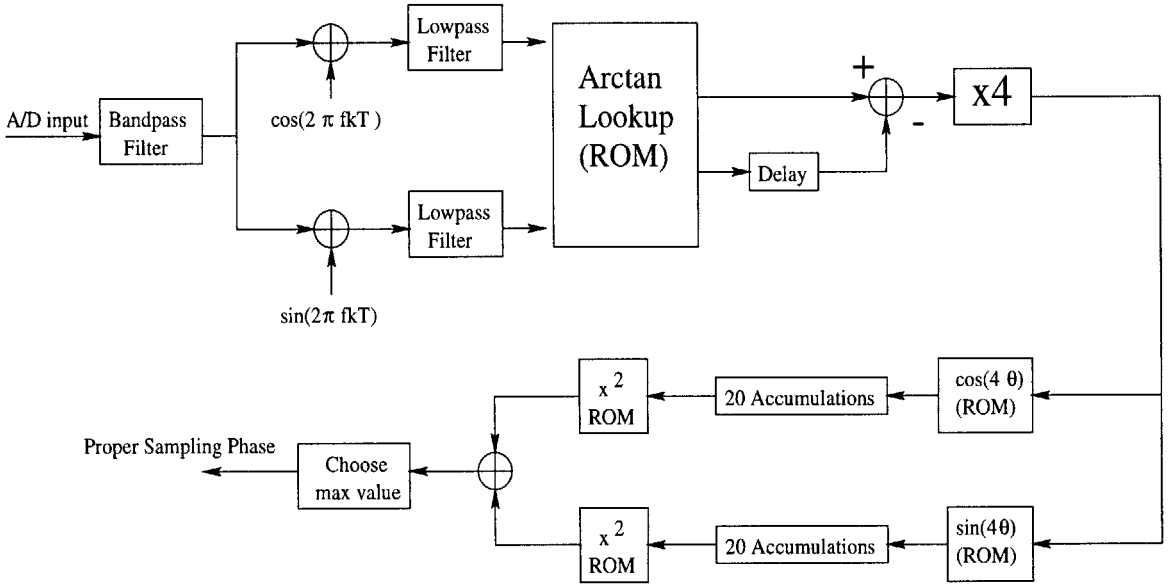

Figure 2-3: Block Diagram of Bandpass-to-Phase portion of the Circuit

The PACS demodulation algorithm begins with the received continuous signal at an intermediate frequency of 10.7 MHz. An A/D converter digitizes this signal with a sampling rate of 3.84 MHz. Because the signal contains frequency components greater than the Nyquist rate, the sampling causes aliasing in the signal. The resulting sampled signal appears to be at 820 kHz. Sampling at this smaller frequency can be thought of as down-conversion using the third harmonic of the sampling frequency, which in effect is a high-side injection with an associated phase inversion.

At this point, although the signal is at 820 kHz, the remainder of the circuit is clocked at 960 kHz, resulting in a bulk frequency offset of 140 kHz. This offset is a compromise resulting from a series of filter design decisions that sought to optimize the filter coefficients to eliminate the need for multipliers in the digital circuit.[1] The performance degradation

[1]There is some advantage to choosing 3.84 MHz as the sampling frequency because it is easy to create

this offset causes is negligible and has been confirmed by experiment to be acceptable, and as shown in Section 2.2, this constant phase offset has no effect on the remaining analysis.

The digitized signal is then passed through a bandpass filter to suppress DC components and quantization noise outside the desired passband [2]. The filtered signal is digitally mixed with sine and cosine carriers at 960 kHz, and two low-pass filters eliminate the double-frequency components of the in-phase and quadrature (I and Q) components of the received signal. Using an arctangent function, the I and Q components are translated into phase information. The difference of the phases of consecutive symbols is taken to obtain the differential phase. Recall that the $\frac{\pi}{4}$-shifted QPSK modulation scheme employed by the transmitter ensures that the difference between the phase of two consecutive received symbols is one of four differential phases, $\pm\frac{\pi}{4}$ or $\pm\frac{3\pi}{4}$. The differential phase is then quadrupled to remove modulation [2]. This quadrupled differential phase is passed to the remainder of the demodulating circuit.

2.4 Symbol Timing

The symbol timing stage of the circuit plays a critical role in this study. The need for symbol timing is a result of the fact that the incoming signal is 20x over-sampled and may experience an unknown delay in transmission. It becomes necessary to choose the correct sampling phase in order to demodulate the signal reliably. Once the symbol timing portion of the system has established the proper sampling phase, every twentieth sample is sent to the remainder of the system to be demodulated.

Symbol timing is achieved by comparing a quality metric that indicates the maximum average opening of the eye-pattern of the signal at each sample phase; the phase with the "best" metric is chosen as the proper sampling phase. Figure 2-4 demonstrates what is meant by average eye opening. When the signal is sampled at the incorrect phase, the eye diagram will reveal an increasingly smaller opening, corresponding to signal distortion due to ISI. However, at the correct sampling phase, the eye diagram should reflect the clear separation of the I and the Q rails. This corresponds to the ideal sampling phase.

This method of selecting the proper sampling phase has demonstrated high performance.

---

that clock from standard crystal oscillators. 960 kHz is precisely one fourth of the sampling frequency. This makes it easy to divide the sampling clock to use for the remainder of the circuit.

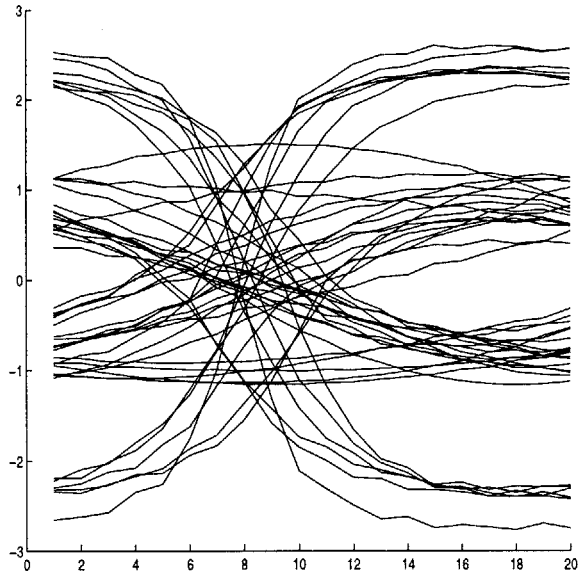

Figure 2-4: An eye-diagram: the sampling point that produces the largest eye-opening is the one closest to the correct sampling phase.

This suggests that this quality metric, or a similar one, may be used to indicate the quality of the overall signal as well. While the eye separation is an indication of the amount of ISI (minimal ISI indicates proper sampling phase) distorting the signal, any type of noise can also distort this eye opening and degrade the system's ability to achieve accurate symbol timing. Therefore, the quality metric used for symbol timing also inherently includes the effects of other types of noise. This suggests that this metric may be useful in performing diversity selection in addition to symbol timing. The desire to increase the efficiency of the circuit by extracting additional performance from the current hardware and design provides sufficient motivation to pursue this possibility.

Chapter 3

Objective: Estimating SNR on a Wireless Channel

We want to develop effective methods to compare the different noise levels of two wireless channels. There are two types of comparisons that will be useful. One is a relative comparison of the noise levels of the two channels for purposes of diversity selection. It is important to the quality of the signal to receive it over the channel with the least amount of noise and interference. However, it is also useful to estimate the absolute level of the noise of a given channel. The PACS standard specifically states that the phone demodulator must be able to estimate within ± 3 dB the actual SNR level in the channel over which it is receiving the signal. It is certainly desirable to be able to guarantee a certain level of quality of service. For instance if a call cannot be received over a channel with a minimum SNR level, it should be dropped in order to maximize the system's resources.

3.1 Objective

One of the primary components of the PACS system is the demodulating algorithm. Data is modulated onto a carrier using $\frac{\pi}{4}$-shifted QPSK modulation with Nyquist square-root of raised-cosine spectral shaping. The data is then recovered using a low-overhead burst-coherent demodulation technique. The demodulator has several functions that contribute to the demodulation. A full description of the system can be found in Chapter 2. Once again, a key advantage of this implementation is the joint estimation of the symbol timing phase and the carrier frequency offset, described in Section 2.4. The demodulator also

employs a diversity selection technique that is based on a quality measure derived as part of the symbol timing/frequency offset estimation process.

Performing diversity selection as a "consequence" of the symbol timing/frequency offset estimation process provides an efficient manner of increasing the performance of the algorithm; furthermore, simulations have shown that this technique presents performance advantages over the traditional method of diversity selection based on power and is almost as effective as diversity selection after channel decoding [1]. The method is founded on the premise that a channel quality metric derived as part of the algorithm can indicate the "noisiness" of the channel.

The effectiveness of this method has been verified in both simulations and laboratory hardware experiments. However, while the utility of this method has been confirmed, its accuracy has not been adequately determined. Also, only its effectiveness as an indicator of relative SNR levels between diversity branches or different symbol timing candidates has been demonstrated; it has not been shown to explicitly convey information about the absolute level of SNR. Establishing a method of quantitatively estimating SNR in the channel can provide improvements in both physical-layer signal processing and higher-layer link management protocols that rely on physical-layer measurements.

The aim of this thesis is to establish the reliability of the quality metric as an indicator of SNR in a channel and to determine its ability to convey specific information about SNR levels. Clearly, part of the objective includes selecting the least noisy channel without incurring heavy costs in terms of additional hardware or computational complexity. In order to optimize efficiency, emphasis has been placed on seeking methods that might be able to incorporate the channel selection method into the demodulation by establishing a clear relationship between SNR and a quantity derived from the demodulation process.

3.2 Experimental Models

All simulations and conclusions in this thesis will assume an additive white Gaussian noise channel model. This is simulated by adding complex Gaussian noise the input signal. That is, we let the noise, $n = x + iy$, where x and y are independent, identically distributed Gaussian random variables. The variance, $\sigma_{x,y}^2 = \frac{\sigma_n^2}{2}$, of x and y is determined by the signal-to-noise (SNR) level in the channel (in dB) as follows: $\sigma_n^2 = 10^{-\frac{SNR}{10}}$. This complex

Gaussian noise is added to the transmitted signal and undergoes the same treatment at the receiver end as the actual signal. The goal of this study is to characterize the effects of this additive noise on the signal.

Once the channel is characterized and the behavior of the hardware can be simulated effectively, then it remains to establish several metrics which will indicate the "quality" of the signal. Our hope is that the signal quality will be directly related to the channel noise. This is a reasonable expectation, since noise clearly degrades the signal. However, it is important to note that noise may not be the only factor that affects signal quality. In this study, it will be assumed that these other effects are either negligible or independent of the channel noise.

If the noise level can be correlated to the value of a metric, a form of statistical estimation based on the metric can be established and become the basis of symbol timing selection, diversity selection, and frequency channel selection and link maintenance. This study will focus on determining if a metric can be developed that is useful for diversity selection. If its utility in this respect can be shown, it will be assumed, but not explicitly shown, that it can also be adopted to perform these other functions.

As described in Section 2.4, the current quality metric is derived from the in-phase and quadrature components of the transmitted differential phase. This is a likely candidate because it represents the phase information that is central to the demodulation algorithm and can be integrated easily into the demodulation process. It also effectively indicates the average eye opening of the eye-pattern of a burst. Furthermore, if the effectiveness of this metric can be determined, it may be possible to derive alternative metrics which may offer greater precision or accuracy.

The following subsections will offer a discussion on the derivation of the metric based on the in-phase and quadrature components and will provide an explanation as to why this metric presents itself as a reasonable indicator of noise. The introduction of an alternative metric will also be made with a brief comparison of the two. A more vigorous comparison will be given during the analysis and results sections.

3.2.1 Quality Metrics

Ideally, with no noise present and zero frequency offset from any source, the received differential phase multiplied by four yields $\pm\pi$ or $\pm 3\pi$, all of which collapse to π. That is,

$$\Delta\theta_i = 4(\theta_i - \theta_{i-1}) = \pi \tag{3.1}$$

Therefore, the quadrupled differential phase provides an absolute ideal phase value, π. Furthermore, the in-phase component is at its maximum magnitude of 1, and there is no quadrature component.

Noise and residual and bulk frequency offsets cause the actual value to deviate from the ideal. Recall, the system undergoes a bulk frequency offset of 140 kHz, causing the ideal phase to actually be: $\Delta\theta = \pi - 4 \cdot 2\pi \cdot f_{off} \cdot T$, where f_{off} represents the bulk frequency offset of 140 kHz and $T = 3.84$ MHz, the sampling period.

Any additional deviation can be thought of as representing the various forms of impairments experienced by the system, such as noise and intersymbol interference. The greater the noise level, the larger the deviation from the ideal. Assuming an ideal sampling phase and minimal ISI, the deviations represent only noise and interference other than ISI. However, the deviation of a single symbol does not provide a precise measure of the noise level because noise and interference may introduce random errors at any sampling phase. Rather, it is more accurate to use a block of symbols and to average the error over this block in order to average out these random errors. Assuming that the channel conditions do not vary widely over the length of one burst (60 symbols), a burst can be used as a block of symbols. By accumulating over the center N symbols of a burst, we avoid symbols from the beginning and the end of each burst which may be affected by the signal ramping up or ramping down due to the filtering. With a sufficiently large N, where we take N to be the 47 center symbols in a burst, the "signal-to-impairment" ratio is maximized at the ideal sampling phase [3].

Note that although this discussion has included the effects of the bulk frequency offset, in reality the analysis that follows is unaffected by this additional bias. Compensating for this bulk offset so that we still deal with an ideal differential phase of π simplifies the analysis and has no bearing on the noise since the effects of the random noise and this bulk offset are separable. Similarly, we can also subtract this bias of π, so that what remains

is a zero-mean variable. For this reason, the remainder of the discussions will refer to an ideal quadrupled differential phase $\Delta\phi$, whose ideal value is zero, referring to an unbiased version of the differential phase, where

$$\Delta\phi_i = 4(\theta_i - \theta i - 1) - \pi. \tag{3.2}$$

Each $\Delta\phi_i$ is a zero-mean Gaussian with variance $16\sigma_n^2$, where non-adjacent $\Delta\phi$'s are independent. However, adjacent phases are dependent. For example, $\Delta\phi_i$ is correlated with both $\Delta\phi_{i-1}$ and $\Delta\phi_{i+1}$ but independent of any $\Delta\phi_j$ for any $j \neq i-1, i, or i+1$.

QI

The actual metric, called "QI", is derived from the in-phase and the quadrature components (the I and the Q) of the phase. Specifically, it is the sum of the in-phase components squared, added to the sum of the quadrature components squared,

$$QI = (\sum_{i=1}^{N} \sin(\Delta\phi_i))^2 + (\sum_{i=1}^{N} \cos(\Delta\phi_i))^2 \tag{3.3}$$

which is effectively the squared magnitude of the sum of the N symbols. The QI essentially represents the cumulative magnitude of the phase deviation and can indicate the "signal-to-impairment" ratio. The phase of this resultant vector should approximate the average of the N individual differential phases.

Summing a block of unit length vectors with an ideal phase, $\Delta\phi = 0$ would yield a larger vector pointing in the same direction. This is illustrated in Figure 3-1 (a). However, noise and residual frequency offset due to differences in the carrier frequency references between the transmitter and the receiver cause the phases to fluctuate around the "ideal" phase so that $\Delta\phi' = \theta_{noise} + \theta_{off}$, where θ_{noise} and θ_{off} represent random errors. Now, instead of N angles all equal to $\Delta\phi$, there is a set of angles $\{\Delta\phi_1', \Delta\phi_2', \ldots, \Delta\phi_M'\}$, where the elements are uncorrelated random variables. However, the resultant vector sum over a block of N symbols could be viewed as approximating the "average" of these vectors, as shown in Figure 3-1 (b).

The sampling phase with the largest magnitude would signal the most accurate phase. Indeed, it has been observed and demonstrated in simulations, that there is an increasing

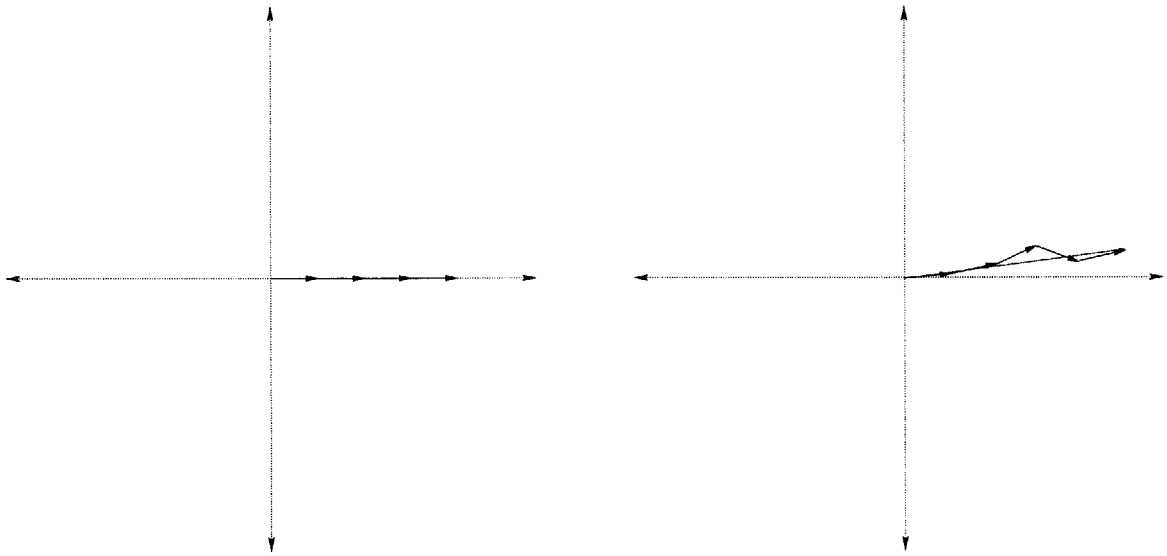

Figure 3-1: (a) Ideal Phases: Vectors line up perfectly. (b) When the individual phases vary, the resultant vector has a phase that is the "average" of the composite phases.

monotonic relationship between SNR and the magnitude of QI. This result suggests that some significant relationship may exist between the two factors, and that the QI may be used as an estimator of SNR level. However, as the SNR becomes large, this best QI will approach a fixed value of N, so QI may not be a very sensitive indicator of SNR when the SNR is large. We will therefore investigate another quality metric which may be a more sensitive indicator of SNR.

Differential Phase

It may also be possible to reveal a useful correlation between SNR and the differential phase error itself. Ideally, the quadrupled phases will always wrap around to π . Any deviation from π will be due to channel noise, ISI, or quantization noise. ISI and quantization noise are negligible at the correct sampling phase and can be ignored for the present time, although it is important to note that their contribution may still be non-trivial. A second metric, the differential phase error (DP), can be defined as variance of the deviation of the quadrupled differential phase from π.

$$DP = \sum_{i=1}^{N} \Delta\phi_i^2. \tag{3.4}$$

The smallest error indicates the phase closest to the correct sampling phase. An illustration of the differential phase variance is given in Figure 3.2.1.

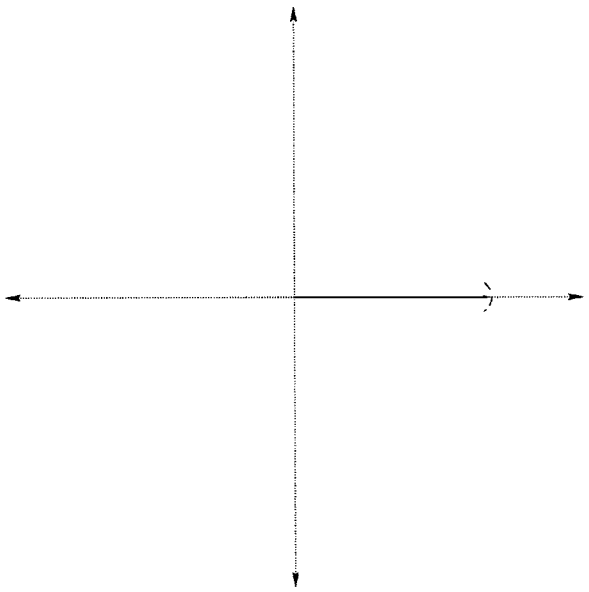

Figure 3-2: Differential Phase - measure the deviation from the ideal $\Delta\phi = 0$

QI and DP are similar since the QI represents the two rectangular coordinates of the differential phase. The relationship between differential phase and SNR resembles the one described above for QI; in fact, it is the inverse. Therefore, it appears reasonable to compare the performance of these two metrics. They have a similar relationship to SNR and represent similar information in two different forms. QI is already in place as a quality metric in the current design of the demodulator; however, if DP is shown to offer performance advantages, the additional computation will be minimal, particularly since the calculation of QI and the calculation of DP have significant overlap.

In fact, there is reason to believe that DP may be a better measure of the noise. As SNR levels get larger, the ability of the QI metric to distinguish between levels weakens. The averaging effects of the vector summation will cause some loss of sensitivity. At close SNR levels, a direct representation of the differential phase itself may be able to yield finer distinctions.

3.3 Phase Jitter

Both QI and DP are dependent on the amount the differential phase of two adjacent symbols deviates from some "ideal" phase. This deviation of the quadrupled differential phase from π is called the "phase jitter" and can be considered to be due to perturbations in the system.

Specifically, DP measures the variance of that "jitter". The mean of DP is expected to be zero, that is zero "jitter" from the ideal phase. The smaller the variance, the less disturbance the signal is assumed to undergo. Similarly, QI measures the projection of the phase angle onto the real axis. Therefore, larger values of QI indicate a phase closer to the ideal phase, or small "jitter", and corresponds to lower noise levels.

Given these relationships, it is clearly advantageous to be able to approximate what the expected variations will be. These calculations will confirm the real data collected through the modeled channel. If the two sets of data do match, that will verify the model and also provide a means on which to base an estimation technique to determine the noise levels.

3.3.1 Approximations to the Probability Distribution of the Phase Disturbance

The detection method being developed in this study is based purely on signal phase information and employs maximum likelihood detection based on the signal phase in the presence of noise. The model approximates the combined effects of ISI, noise, and interference as a Gaussian process and aims to measure the phase disturbance of the signal due to different levels of interference. It is known that such a phase disturbance of a received waveform in complex Gaussian noise has a probability density function (pdf) given by:

$$p(\theta) = \frac{1}{2\pi} e^{-\gamma}(1 + \sqrt{4\pi\gamma}\cos\theta e^{\gamma\cos^2\theta}\frac{1}{\sqrt{2\pi}}\int_{-\infty}^{-\sqrt{2\gamma}\cos\theta} e^{-\frac{x^2}{2}}dx) \tag{3.5}$$

where γ is the SNR per symbol ($\gamma = \frac{1}{\sigma_n^2} = 10^{\frac{SNR}{10}}$) [7]. Figure 3-3 displays $p(\theta)$ for several values of γ. Clearly, as γ increases, corresponding to increasing SNR, $p(\theta)$ becomes narrower and more peaked about $\theta = 0$. This represents a phase "jitter" that approaches zero as SNR increases. This also corresponds to the discussion above, where the variance of DP, around its mean of zero, decreases as SNR increases.

Although the distribution of θ is given in its exact form in Equation 3.5, it is clumsy and

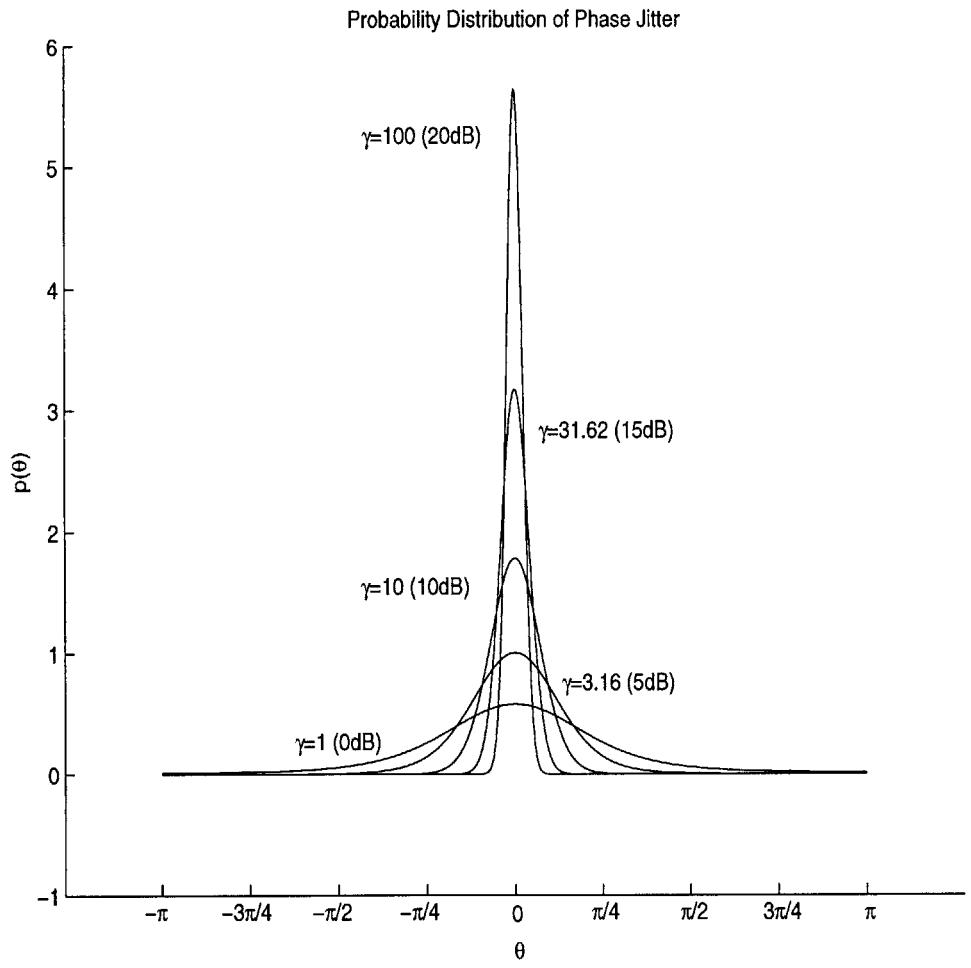

Figure 3-3: Probability density of $p(\theta)$ for γ = 1, 5, 15, 20 dB

difficult to manipulate in calculations. However, we can see that when SNR is large and θ is small, θ is approximately just the quadrature noise component, which is a Gaussian variable of mean zero and variance $\frac{\sigma^2}{2}$. Figure 3-4 illustrates that $p(\theta)$ is well approximated by a zero-mean Gaussian with variance $\frac{\sigma_n^2}{2}$ for SNR values of 10 dB and higher. The analysis in the following section will evaluate how QI and DP are expected to be affected by noise given by this approximation in the specified range of SNR levels.

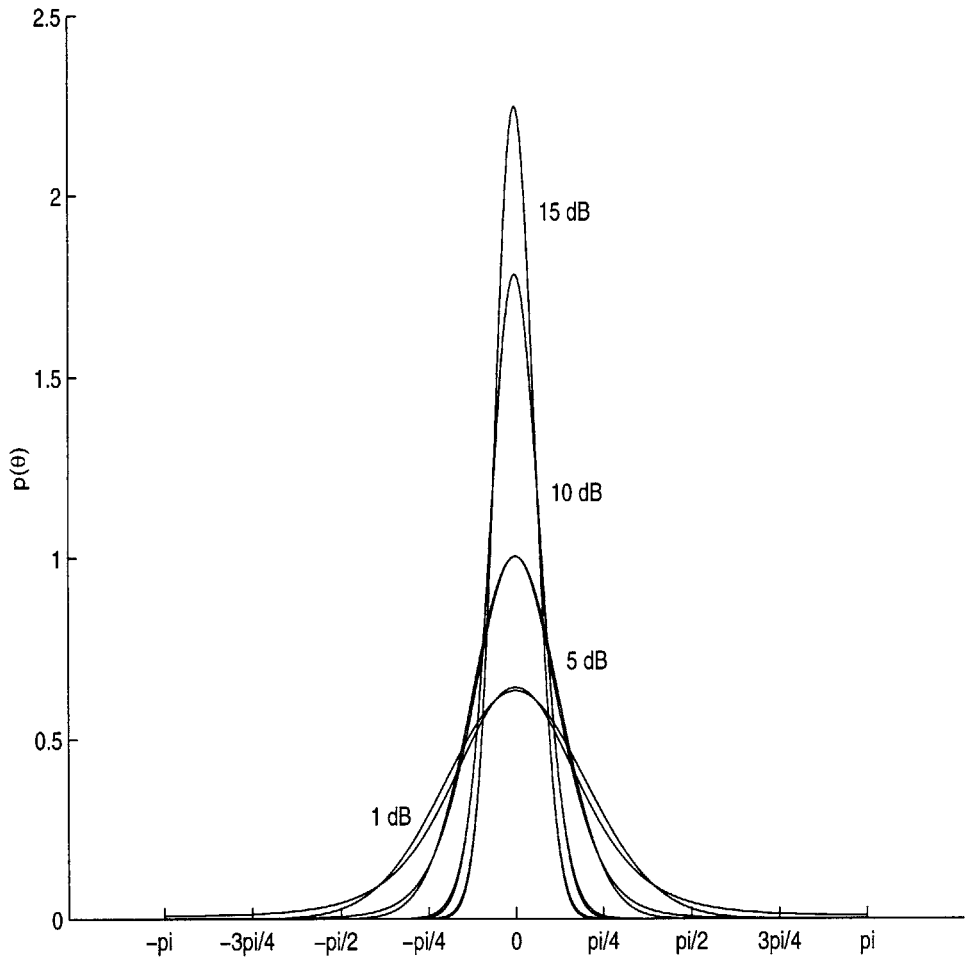

Figure 3-4: Probability density of p(θ) of phase error θ due to additive noise and its approximation function $\mathcal{N}(0,\frac{\sigma_n^2}{2})$

3.3.2 Expected Results

Based on the Gaussian noise-ISI-interference approximation model, it is possible to derive a set of expected results for both QI and DP. Recall that QI is defined as

$$QI = (\sum_{i=1}^{N} \sin(\Delta\phi_i))^2 + (\sum_{i=1}^{N} \cos(\Delta\phi_i))^2$$

where each $\Delta\phi_i = 4(\theta_i - \theta_{i-1}) - \pi$ and θ_{i1} and θ_{i2} each has a probability distribution as given in Equation 3.5. For higher SNR levels, it has been shown that θ, the deviation of the phase from the ideal is small and has a distribution that approximates a zero-mean Gaussian with variance $\frac{\sigma_n^2}{2}$. Consequently, $\Delta\phi_i$, being the scaled sum of two Gaussian random variables, is also another Gaussian random variable with mean zero and variance $16\sigma_n^2$.

Furthermore, because $\Delta\phi$ is expected to be small for higher levels of SNR, $\sin(\Delta\phi_{small})$ can be approximated as $\Delta\phi_{small}$ and $\cos(\Delta\phi_{small})$ can be approximated as $(1 - \frac{\Delta\phi^2_{small}}{2})$. This yields the following approximation for QI, given and SNR level greater than 10dB:

$$QI = (\sum_{i=1}^{N} \Delta\phi_i)^2 + (\sum_{i=1}^{N} (1 - \frac{\Delta\phi_i^2}{2}))^2. \tag{3.6}$$

QI can be viewed as a random variable, and the calculations of both its mean and its variance can be greatly simplified using the approximations derived above.

From Equation 3.6, the expected value of QI (E[QI]) is

$$\begin{aligned} E[QI] &= E[(\sum_{i=1}^{N} \Delta\phi_i)^2 + (\sum_{i=1}^{N} (1 - \frac{\Delta\phi_i^2}{2})^2] \\ &= N^2 - (N^2 - 1)(16\sigma_n^2) + \frac{1}{4}(N^2 + 3N - 1)(16\sigma_n^2)^2 \end{aligned} \tag{3.7}$$

and the variance of QI is given by

$$\begin{aligned} var(QI) &= E[(QI)^2] - E^2[QI] \\ &= (3N^3 + N^2 + \frac{3}{4}N - \frac{31}{4})(16\sigma_n^2)^2 + \frac{1}{2}(-5N^3 - 23N^2 + 11N + 20)(16\sigma_n^2)^3 \\ &+ \frac{1}{16}(9N^3 + 82N^2 + 99N - 208)(16\sigma_n^2)^4 \end{aligned} \tag{3.8}$$

The second-order statistics for DP follow a similar derivation. Recall,

$$DP = \sum_{i=1}^{N} (\Delta\phi_i - \bar{\Delta\phi})^2.$$

Once again, $\Delta\phi$ is zero-mean Gaussian; therefore, $DP = \sum_{i=1}^{N} \Delta\phi_i^2$ and E[DP] can be given as

$$\begin{aligned} E[DP] &= E[\sum_{i=1}^{N} \Delta\phi_i^2] \\ &= 16N\sigma_n^2 \end{aligned} \tag{3.9}$$

and the variance of DP is given by

$$\begin{aligned} var(DP) &= E[(DP)^2] - E^2[DP] \\ &= E[(\sum_{i=1}^{N} \Delta\phi_i^2)^2] - (16N\sigma_n^2)^2 \\ &= (3N-1)(16\sigma_n^2)^2 \end{aligned} \tag{3.10}$$

These are the expected results for QI and DP. It will be demonstrated in Chapter 5 that these match closely with the actual results, within this range of interference, confirming the Gaussian approximation to Equation 3.5. Using these values, it is possible to detect maximum likelihood SNR level present in the channel, for SNR levels of 10 dB and higher. Unfortunately, similar results for smaller SNR levels is not available.

Chapter 4

Experiments

Quantitative data can confirm the theoretical results developed in Chapter 3. For the purposes of analysis, it is preferable to avoid complications that may occur from generating and using a data set taken from an actual handset. Rather, data generated from simulations in a controlled environment can be analyzed and used to develop a reasonable model which can be extrapolated to approximate real behavior. Therefore, it is important to develop experiments that accurately reflect the behavior of a real-time system and that consider the major issues that will impact the real data. The following chapter will describe the development of such an experiment and will also discuss some of the simplifications and modifications made in order to aid analysis of the data.

4.1 Design of The Experiment

The design of the approach used to study the observed behavior of the metrics in the demodulating algorithm was based on the assumptions and analytical results detailed in Chapter 3 and can be divided into two levels. The first level is the simulation of the hardware and the modeling of the Gaussian channel to generate data. The second level is an analysis system to characterize the data using many probabilistic concepts and taking advantage of the forms of many random variables which can be reasonably presumed from the discussions in previous chapters.

Simulations of the system behavior at the hardware level were designed in Matlab. In this way, a random sequence can be generated to create a signal similar to one that would be transmitted under ideal conditions; complex additive white Gaussian noise is added to

simulate how the signal would be distorted under an actual channel, according to our model. The signal then undergoes demodulation according to the PACS algorithm. The I and the Q information is extracted at the end of the bandpass-to-phase portion of the circuit, and QI and DP are calculated. If a large set of QI and DP samples are collected for various channel conditions, then statistical analysis can be performed on the data characterize the expected behavior of the metrics.

4.2 Hardware Simulations

The first level of the experiments involves simulating the hardware implementation of the PACS system to generate a data set to use for further analysis. Essentially, this behavior follows that described by Figure 2-3 and in Section 2.3. A copy of the Matlab file that implements this procedure can be found in Appendix A.

The demodulator expects to receive an input signal that has been encoded by the transmitter with a $\frac{\pi}{4}$-shifted QPSK modulation scheme and that has experienced a random amount of interference in the channel. To simulate the transmitter, a random differential phase sequence is generated and used to derive the actual phases for a random encoded signal. This sequence is altered to resemble a 20x oversampled signal, as specified by the PACS transmitter design. Typically, the transmitter will filter the signal with a square-root of raised-cosine shaping filter to help reduce ISI. Once the signal has been transmitted, additive white Gaussian noise is added to simulate signal distortion under an actual channel. A square-root of raised-cosine receive filter identical to the transmit filter shapes the incoming signal in an attempt to remove some of the noise and to reduce ISI. The signal is then down-sampled to 820kHz and mixed with sine and cosine functions to generate the I and the Q rails. These are then translated into phase information via inverse tangent functions and differenced to retrieve the differential phase information. The differential phase is quadrupled to remove modulation, and at that point, the simulations will diverge from demodulation and begin to generate the metrics of interest.

Equation 3.6 describes how the QI metric will be constructed. Recall that the signal is 20x oversampled. Therefore, a QI value must be calculated for each of the 20 different sampling phases. Once all twenty QI values have been calculated, the phase with the highest QI value is chosen, and that index represents the proper sampling phase. The same will be

done for the DP metric at each of the twenty sampling phases. However, in the DP case, the smallest of the twenty values is chosen to represent the metric.

4.2.1 Issues and Modifications to the Model

It is important to note that while these simulations attempt to accurately reflect what happens in the hardware, simplifications to the actual logic design included several quantization steps. For instance, lower order bits were often truncated, and transcendental and algebraic functions were performed using look-up tables with fixed-length outputs. Extensive testing has been performed to determine what level of quantization yields acceptable results with minimum degradation in probability of symbol error as a function of SNR. However, the non-linear nature of such simplifications complicates analysis of the underlying algorithms. Therefore, for the purposes of this study, "unquantized" simulations have been used. That is, all look-up tables are eliminated and replaced with full machine-floating point accuracy for all variables. Although the data will not reflect the actual values produced by the hardware, the analysis presented here will nonetheless provide important insight into how the signals are affected by channel noise. These results can be adopted to account for the quantization effects ignored here.

4.3 Establishing a Data Set

Following the method described Section 4.2, it is possible to derive a QI and a DP value for a particular signal. However, data from a large number of trials is needed to be able to develop a statistical characterization of the metrics. Therefore, random data will be gathered through Monte Carlo simulations under various channel conditions. Specifically, SNR levels of 0 dB to 30 dB will be simulated with 0.5 dB increments; 1000 bursts, each 60 symbols in length, will be run through the simulated demodulator at each SNR level. Given a large enough set of simulations, the data collected will represent a random set whose average behavior should approximate the metric's distribution.

4.4 Statistical Analysis of Data

The second level of the experiments is to devise a method to analyze the results drawn from the experiments described above. One of the first things to investigate is the general rela-

tionship between the metrics and SNR. The most immediate observation is the monotonic relationship between the QI and the SNR levels. This relationship is illustrated in Figure 4-1. QI increases with increasing SNR; this suggests that a low QI implies a low SNR. DP exhibits similar behavior, with an inverse relationship to SNR, as expected. It is clear that the effects of noise do, indeed, reduce the demodulator's ability to extract the correct symbol timing phase and will directly impact the value of the metrics' as measures of the channel noise. The important question, however, is how high is the correlation between channel noise and the metrics and which of the two metrics is more closely correlated to SNR. Once that is determined, it will remain to evaluate how that metric can be used to convey additional information about the channel noise.

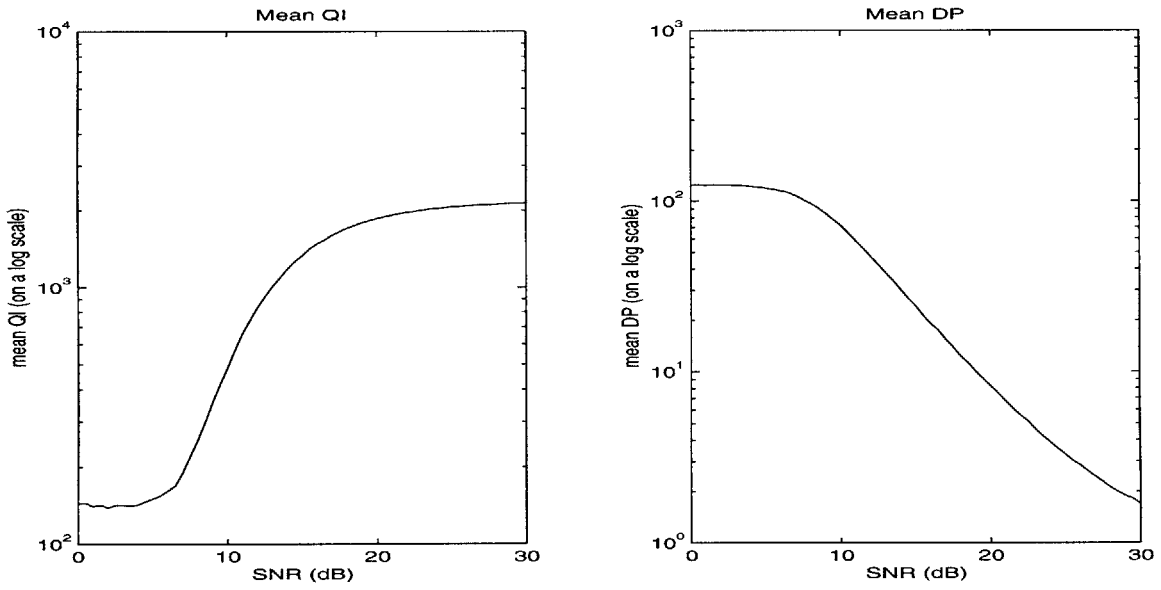

Figure 4-1: Plot of Mean QI and Mean DP Values over SNR levels from 0dB to 30dB

Furthermore, it is pertinent to use the simulated data to verify the models developed in previous chapters. As detailed in Chapter 3, the expected phase jitter can be modeled as having a Gaussian distribution for SNR levels greater than 10 dB. Section 3.3.2 derives the expected results for both the QI and the DP using this approximation. Verifying that the simulated and the expected results match will confirm the model and the results.

4.4.1 Deriving Distributions and Goodness-of-fit Testing

Once a relationship between the metrics and SNR has been established and their expected behavior has been verified, further characterization of the metrics is possible. The second-

order statistics discussed in Section 3.3.2 and Section 4.4 help to derive and verify the probability densities of the metrics conditioned on a given SNR level. Using the **hist** function in Matlab, it is possible to bin the values of a vector of experimental data and to plot a bar graph representing the distribution of the random variable. An example of this binning is shown in Figure 4-2. Using this data, it is possible to test for particular

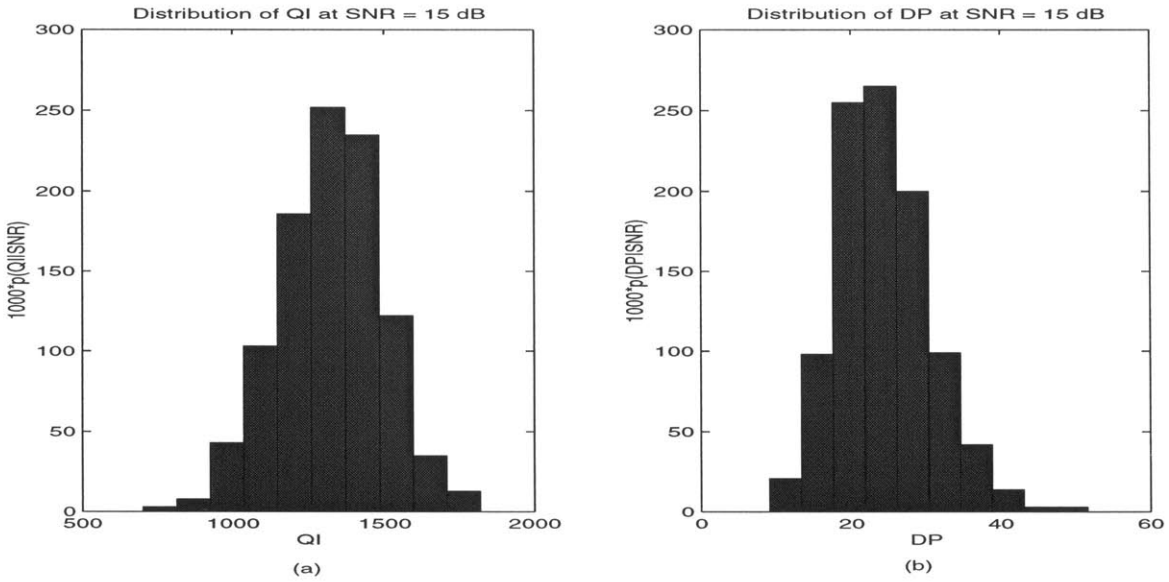

Figure 4-2: Sample Histograms of QI (a) and DP (b) samples at SNR = 15 dB

distributions.

Goodness-of-fit testing methods have been developed to provide a means to confirm the suspected distribution of a particular random variable. Both QI and DP can be treated as random variables with some unknown distribution. The Monte Carlo simulations provide us with observations of the the metrics at particular SNR levels. The means and the variances can be calculated empirically, and goodness-of-fit testing can be used to confirm a distribution using these second-order statistics. [9] documents the method of testing followed in this study. Using the binning information derived from the **hist** function, it is possible use these methods to test for particular distributions.

Accurately characterizing the distributions of the metrics is crucial to continuing statistical analysis on the data. Knowing the distribution of the metric, there are many well-defined methods of estimating SNR from a given QI or DP value that can be applied. For instance, if the distribution is unimodal, then we can use maximum likelihood estimation techniques to formulate a mapping between SNR levels and particular metric values.

4.4.2 Discriminating Between SNR Levels

Finally, a measure of a metrics' ability to successfully discriminate between two different SNR levels is difficult to capture. From the sections above, we know that we can calculate the mean and standard deviation of each metric as a function of SNR. For a given SNR level, we can define the expected range of that metric to be its mean plus or minus one standard deviation. This should represent the range in which the majority of the probability density falls; that is, it represents the most likely values the metric will take on given that the channel conditions are as defined by the particular SNR level.

In this way, two SNR levels are "distinguishable" if their expected ranges do not overlap. The distance between distinguishable SNR levels will vary for each metric. Clearly, one metric is better than the other if it distinguishes between two SNR levels that are indistinguishable by the other.

Evaluating the metrics in this manner makes some statement on its ability to perform diversity selection. If the expected ranges are too large, the ability to discriminate between nearby SNR levels is hampered. Likewise, if the means at different SNR levels are too similar, this may also inhibit the metrics' ability to distinguish between levels. Therefore, a metric with distinct means for each SNR level and small variances will exhibit a greater ability to perform diversity selection.

Chapter 5

Results

Following the methods described in Chapter 4, a set of random QI and DP data was established at 61 different SNR levels (for SNR=0 dB to SNR=30 dB with 0.5 dB increments). Statistical analysis was performed on the data, and the results are presented in this chapter. This presentation will include a characterization of the data, where the possible probability distribution of the metrics are discussed. If a suitable distribution can be verified, the metric will undergo further analysis according to the experiments detailed in Section 4.4. For instance, it will be shown how the data can be used to derive information about the SNR level given certain assumptions. Finally, a treatment of the expected performance of these metrics will be offered. The following chapter will discuss some conclusions based on these results and propose several suggestions and possibilities for further or future work in this area.

5.1 QI

The simplest way to begin a classification of the distribution of QI is to calculate the empirical means and standard deviations of the metric at particular SNR levels. This is easily done in Matlab using the test vectors generated by the Monte Carlo hardware simulations described in Chapter 4. Plots of the calculated means and the calculated variances of QI against a log scale of the dB levels at which they were measured is shown in Figure 5-1. Several things are observable from these plots. One is the monotonic relationship between the expected QI and the SNR level in the channel. It is clear that the effects of noise do, indeed, affect QI values in a distinct relationship, and does thereby, reduce the demodulator's

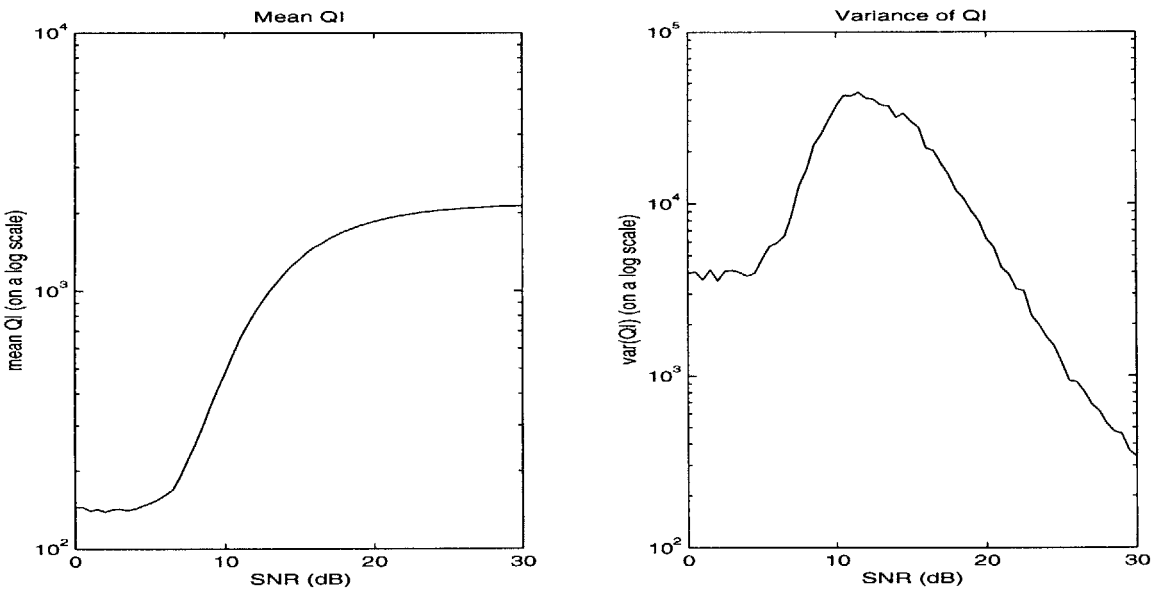

Figure 5-1: Plot of Mean QI Values and its Standard Deviation over SNR levels from 0dB to 30dB

ability to extract the correct symbol timing phase. It is also notable that the QI begins to saturate after a certain SNR level, leading to the belief that a certain amount of degradation occurs from ISI, and not inherently from other sources of noise. These are not effects that were considered as significant in the channel model, and therefore are not included in the analysis. However, they clearly have a role in affecting QI. These effects may reduce the power of the proposed methods in this study, and that degradation in performance will be addressed in the conclusion.

From these plots, it is hoped that QI can be shown to have a direct relationship to SNR, whereby a QI value can give reliable information on the SNR level present on the channel. Note that what is shown in the plots in Figure 5-1 are QI values given a particular SNR level. These correspond to the distribution calculated in Chapter 3. Figure 5-2 demonstrates that the compiled data matches the expected results calculated in Section 3.3.2. Although the curves are not exact matches, they do, indeed, approximate each other. From this, the results derived in Chapter 3 can be considered valid approximations for the range of SNR levels specified.

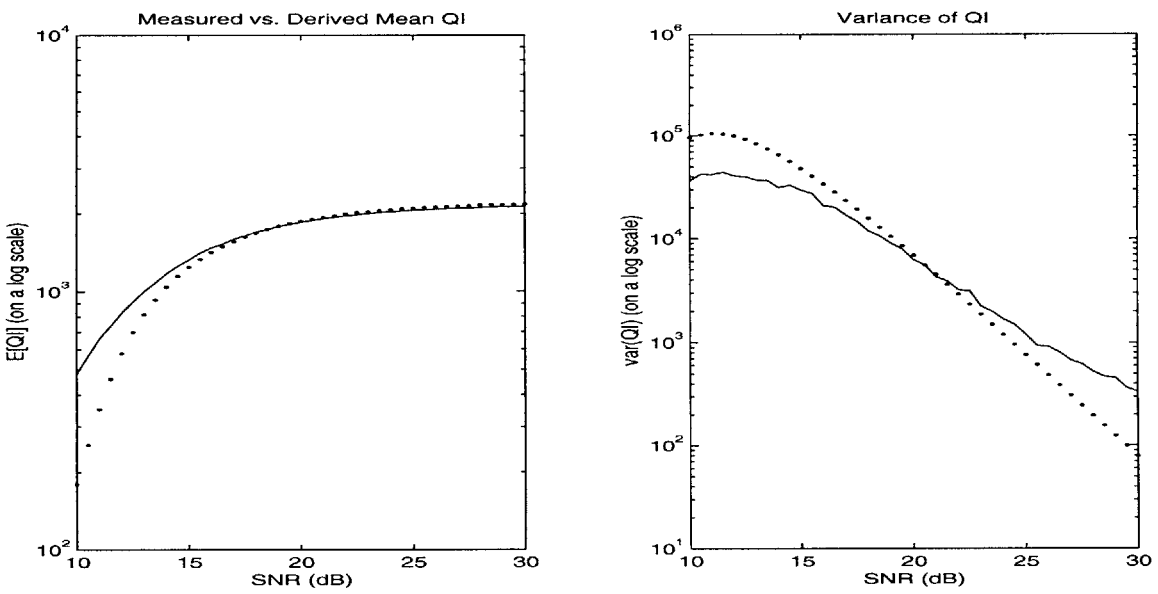

Figure 5-2: (a) Mean QI vs. E[QI] (b) Calculated vs. Derived Variance of QI The solid line represents the measured means and variances of QI's for 1000 different simulations at SNR levels 10dB and higher. The dotted lines are the curves given by Equation 3.7 and Equation 3.8.

5.1.1 Goodness-of-Fit Testing

From the discussion above, a partial characterization of $p(QI|SNR)$ can be derived from the random data sets. Furthermore, Section 3.3.2 derives QI as a combination of $\Delta\phi^4$ and $\Delta\phi^2$, where the $\Delta\phi$'s each have a Gaussian distribution. The higher order terms make it difficult to characterize QI in a form suitable for further statistical analysis. This is unfortunate because without full knowledge of the form of the distribution, it is difficult to evaluate the expected behavior of the metric.

Some goodness-to-fit testing was done to determine if the combined effects of the components of QI might approximate a Normal or a gamma distribution. QI failed both goodness-to-fit tests. Therefore, it is difficult to use analytical methods to form an estimate of SNR from QI. It is possible to continue running Monte Carlo simulations and to form a numerical model of the behavior. However, these will necessarily be subject to the data observed and will rely on the simulations of the models. Hence, although it is not possible to continue with a vigorous statistical analysis, its ability to discriminate between two channels should still be verified. Confirming its reliability in this sense continues to be important, as this is the metric currently used in the system to perform diversity selection. If its reliability can be established, using numerical methods to continue to characterize QI would be a feasible

as the next step.

5.1.2 Ability to Discriminate Between SNR Levels

As described in Section 4.4.2, the ability of a metric to discriminate between different SNR levels is measured by the range of values over which the metric will most likely take on values. The tighter the range, the greater the metric's ability to distinguish between different SNR levels. Figure 5-3 shows a plot of the means of QI with error bars indicating a range of plus or minus one standard deviation. From the figure, it is apparent that the QI's ability to

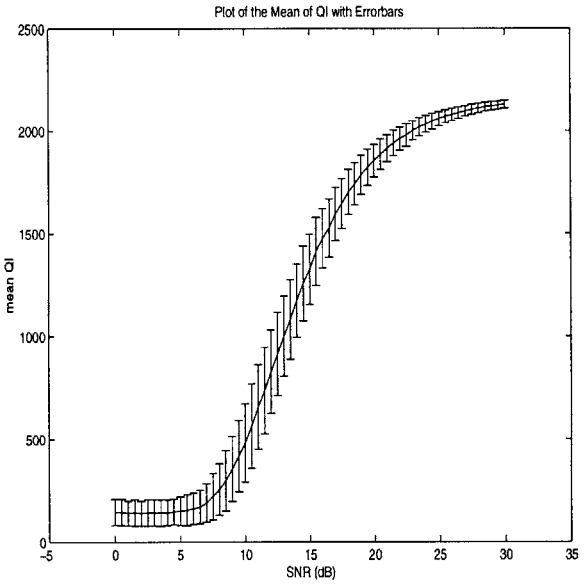

Figure 5-3: Mean QI values with Error Bars to indicate plus or minus one Standard Deviation

discriminate between adjacent SNR levels is pretty low, but the average distance between distinguishable levels is about 3.7 dB.

Figure 5-4 offers a closer view of the ranges, and demonstrates what is meant by "distinguishable" SNR levels by marking some sample distances between distinctly separated SNR levels. Note that from 0 dB to about 5 dB, the SNR levels are virtually indistinguishable from one another. The ranges are almost identical, implying that QI cannot distinguish in any way between those SNR levels. Figure 5-4 (a) shows that the next distinguishable SNR level from any of these is approximately 9 dB. The inability to discriminate between these lower SNR levels may degrade the performance of QI. However, the argument can be made that there is little advantage in accurately distinguishing between SNR levels this low.

Signal quality will be poor enough that the user may not perceive an improvement even if the stronger channel is reliably chose. Accurate diversity selection is more important when choosing between a poor to moderate SNR levels and one that can clearly offer a better quality signal. Figure 5-4 (b) demonstrates that from about 7 dB, shortly after the Mean QI curve begins to increase, the distance to the next distinguishable level is only 3 dB. At more intermediate SNR levels, the distance becomes even smaller, indicating that performance improves in the band of interest. For instance, Figure 5-4 (c), QI can distinguish between SNR levels as close as 14 dB and 16.5 dB.

5.2 DP

Section 3.2.1 introduced a new metric defined by the mean-squared variance of the quadrupled differential phase of the signal. This differential phase metric, or DP, is premised on many of the same concepts as the ones from which QI was drawn. Therefore, if QI was an accurate metric to use in symbol timing, DP promises to demonstrate similar performance. However, where QI was not able to provide easy access to an estimate of SNR, DP may be more robust in this sense.

Once again, analysis of this metric begins with a classification of the distribution by calculating the empirical means and standard deviations of the metric at particular SNR levels. Figure 5-5 depicts plots of the calculated means and the calculated variances of DP against a log scale of the dB levels at which they were measured. Similar to the QI metric, DP has a monotonic relationship between its expected value and the SNR level in the channel, and once again, the metric begins to saturate at higher SNR levels. This is consistent with the idea that some amount of the expected degradation comes from interference sources not included in the model. Figure 5-7 presents a comparison of the empirically determined second-order statistics for QI versus DP. Furthermore, these values seem to correspond well to the approximations shown in Chapter 3. Figure 5-6 illustrates that the empirical results (solid line) follow the analytically derived results (dotted line) well.

Figures 5-7(c) and 5-7(d) illustrate the normalized variance of the metrics, that is the variance normalized by the mean at that particular SNR value. The means demonstrate similar behavior, implying that DP should also offer similar performance. However, from

the plots of the variances, it is interesting to note that the normalized variances of DP are significantly smaller than that of QI. This implies that the DP metric may prove to offer greater sensitivity to the effects of noise. If the DP metric varies less greatly, it's expected value offers a more reliable estimate of the actual results.

5.2.1 Goodness-of-fit Testing

As described in Section 4.4.1, goodness-of-fit testing can verify if a particular variable exhibits behavior that can be characterized by a given probability distribution. In the QI case, we were not able to successfully characterize the distribution. However, DP may offer a simpler analysis than QI, allowing more extensive verification of its utility and a more robust tabulation of it's results. For instance, Section 3.3.2 derives QI as a combination of $\Delta\phi^4$ and $\Delta\phi^2$, where the $\Delta\phi$'s have Gaussian distributions. This does not imply any common probability distribution form. However, DP is a combination of $\Delta\phi^2$. This is a simpler distribution to estimate. A combination of squared Gaussians imply a gamma distribution, given as

$$p_x(x) = \frac{x^{a-1}e^{-\frac{x}{b}}}{(a-1)!b^a}, \tag{5.1}$$

where $E[x] = ab$ and $\sigma_x^2 = ab^2$. Using the calculated means and variances of DP, it is easy to solve for the parameters a and b. Performing goodness-of-fit testing on the DP data verifies that it is distributed according to a gamma distribution. Figure 5-8 depicts a sample histogram of a set of 1000 random DP data points generated at 15dB SNR. From the figure, it can be seen that the distribution of DP resembles a gamma distribution.

From this analysis, we see that DP can be characterized by a distribution with a known form. It is possible to take advantage of the behavior of this form and perform further statistical analysis on the metric. In this manner, we can obtain a concrete model for the expected behavior of the metric. With knowledge of the expected behavior, it is a matter of inverting this relationship to be able to form an estimate of SNR given an observation of DP.

5.2.2 Ability to Discriminate Between SNR Levels

Similar to the analysis described in Section 5.1.2, DP can be evaluated for its ability to discriminate between SNR levels. Figure 5-9 shows a plot of the means of DP with error bars indicating a range of plus or minus one standard deviation. This is analogous to Figure 5-9, and this section will both describe the findings on DP's average ability to discriminate between SNR levels and also compare this performance to that of QI described in Section 5.1.2.

On average, DP can distinguish between SNR levels separated by approximately 3.5 dB. This is very similar to the results derived for QI. Again, Figure 5-10

offers a closer view of the ranges to offer some perspective on its ability to distinguish between SNR levels. Once again, the ranges are virtually indistinguishable from 0 dB to about 4 dB. This is slightly better than the QI performance observed, but not significantly better. However, once again, the argument can be made that these lower SNR levels are less critical than higher ones. Figure 5-10 (a) shows that the next distinguishable SNR level is approximately 8.5 dB. Again, this is only slightly better than the first distinguishable level for the QI. Once we get beyond the lower SNR levels, the performance improves. For instance, in Figure 5-10 (b), the DP can distinguish between 5.5 dB and 9 dB. At more intermediate levels of SNR, it can successfully distinguish between 14 dB and 16.5 dB. This last result is identical to that of QI at the same SNR levels. QI and DP do not seem to differ much in their ability to discriminate between SNR levels.

5.3 SNR Discrimination

It was originally postulated that DP would be able to offer greater sensitivity to the perturbations to the differential phase caused by the noise. It has been shown in the above sections that this is not the case. In fact, QI and DP exhibit approximately the same ability to discriminate between SNR levels. A possible explanation of this can be found in looking at the expected results derived in Chapter 3.

Defining a quantity, D, as the ratio of the mean expected perturbation of the metric from its ideal (QI = $N^2 = 2209$, DP = 0) to the standard deviation of that perturbation. Using the expected results from Section 3.3.2 and assuming large N and large SNR, it can be shown that D approaches $\sqrt{\frac{2}{N}}$. Note that because we are assuming large SNR, the terms

including higher orders of σ_n^2 drop out of the ratio and simplify the computation.

In other words, for QI this would be:

$$\begin{aligned} D_{QI|SNR} &= \frac{(2209 - E[QI|SNR])}{std(QI|SNR)} \\ &\approx \frac{N^2(16\sigma_n^2)}{\sqrt{3N^3((16\sigma_n^2)^2}} \\ &\approx \sqrt{\frac{N}{3}} \end{aligned}$$

Similarly, for DP this would be:

$$\begin{aligned} D_{DP|SNR} &= \frac{E[DP|SNR]}{std(DP|SNR)} \\ &= \frac{16N\sigma_n^2}{\sqrt{(3N-1)(16\sigma_n^2)^2}} \\ &\approx \frac{16N\sigma_n^2}{\sqrt{3N(16\sigma_n^2)^2}} \\ &\approx \sqrt{\frac{N}{3}} \end{aligned}$$

Clearly, the performance of QI and DP are expected to be very similar. They do not demonstrate remarkable differences in their ability to detect perturbations from their ideal values. Instead, they appear to offer very similar expected results. Of course, these approximations are only valid for high SNR, and furthermore, the approximations derived in Section 3.3.2 were also only valid for SNR levels of 10 dB and higher. For lower order SNR, the ability of one metric to discriminate between SNR levels may be higher, but there is no numerical mechanism by which we can measure that. Instead, we will rely on the results of simulations to evaluate their ability at lower SNR levels.

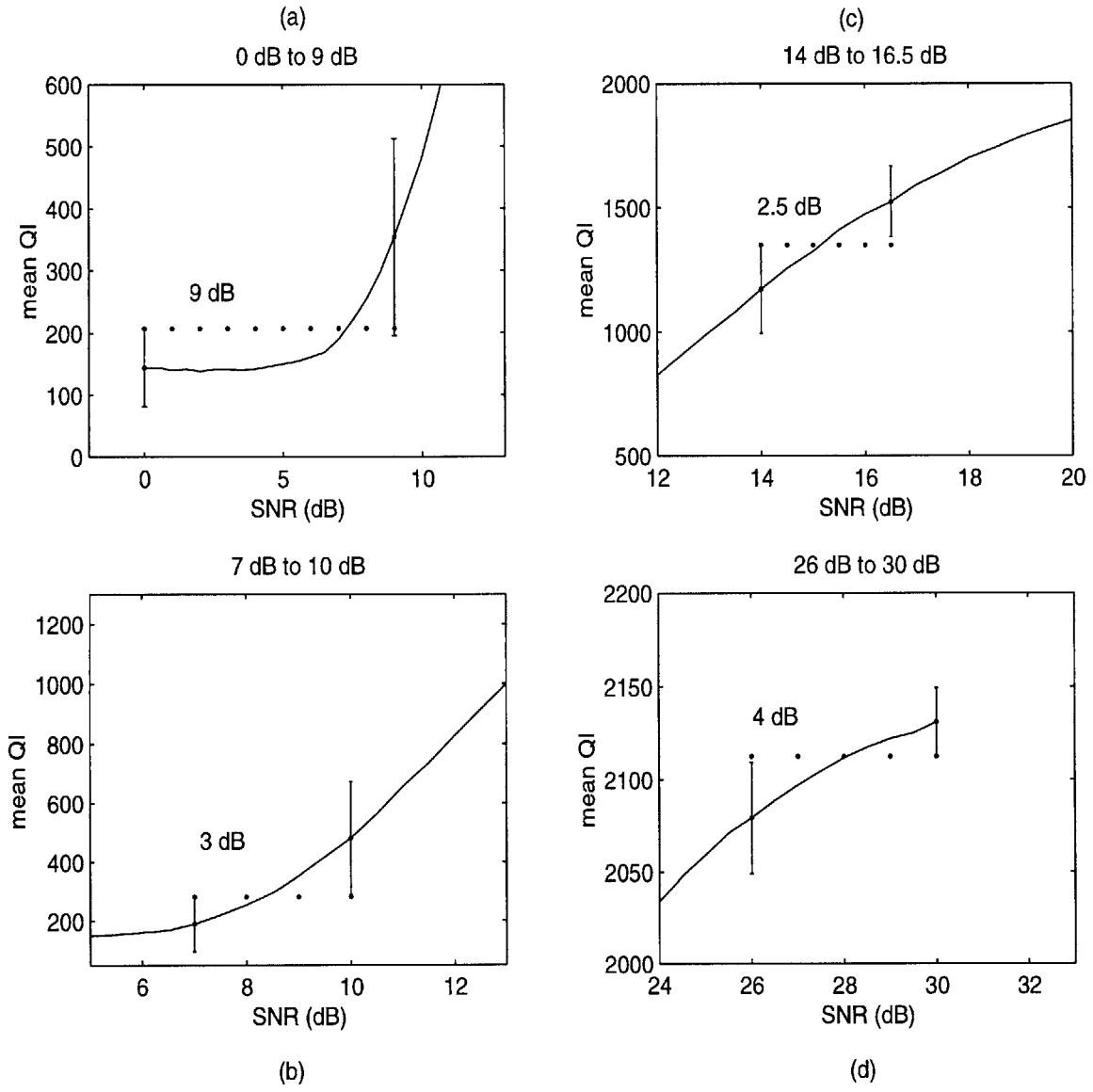

Figure 5-4: Sample Distances Between Distinguishable SNR levels for QI metric

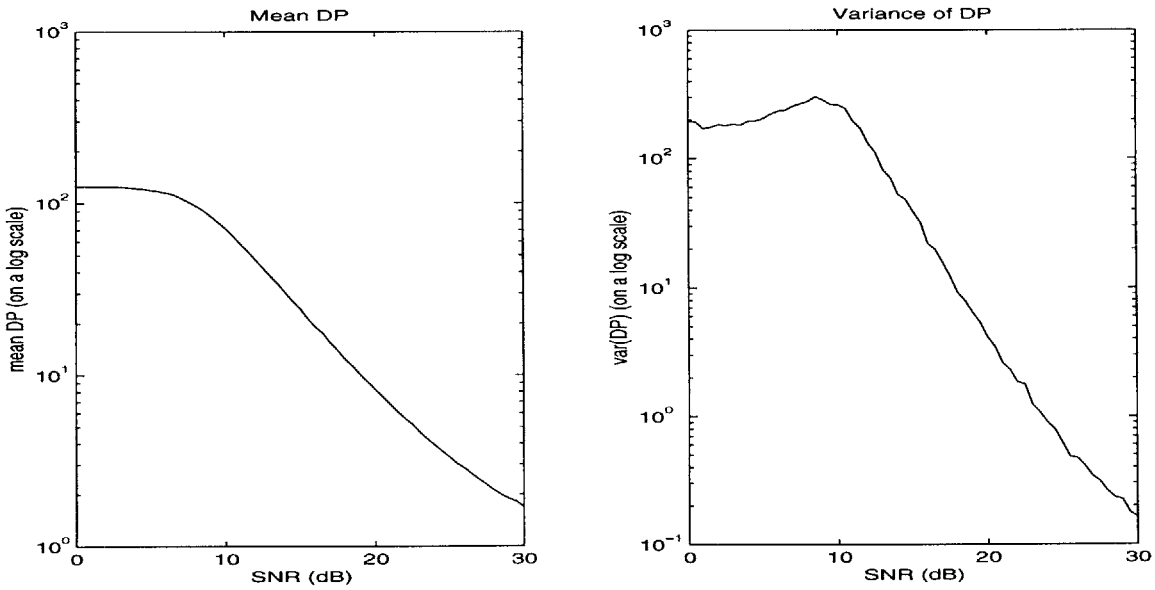

Figure 5-5: Plot of Mean DP Values and its Variance over SNR levels from 0dB to 30dB

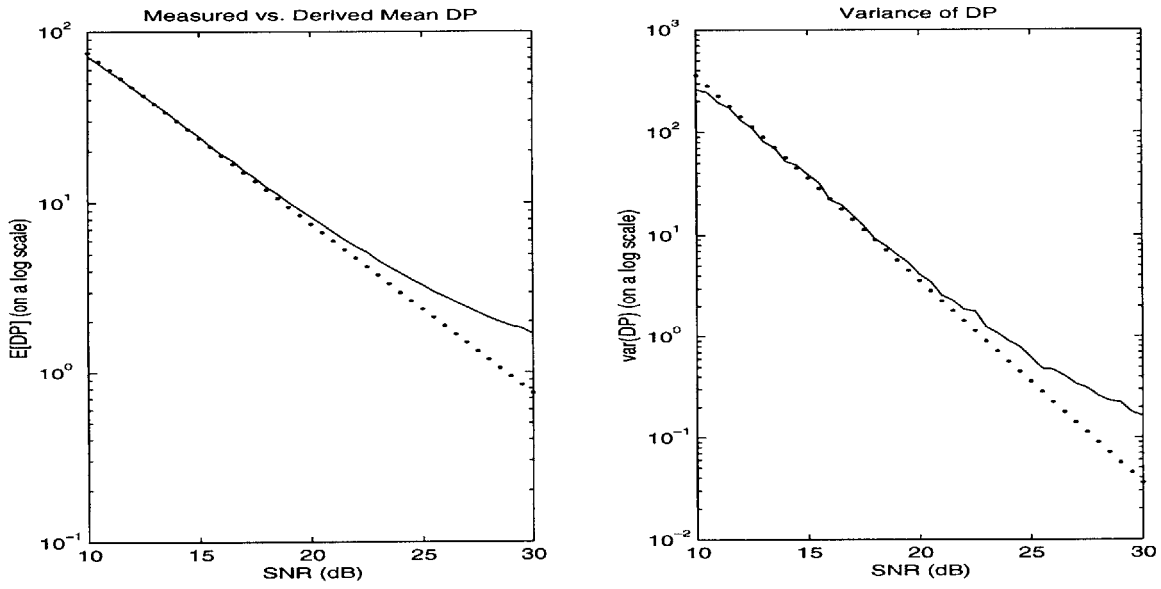

Figure 5-6: The solid line represents the calculated means and variances of DP's for 1000 different simulations at SNR levels 10dB and higher. The dotted lines are the curves given by Equation 3.9 and Equation 3.10. (a) Mean DP vs. E[DP] (b) Calculated vs. Derived Variance of DP

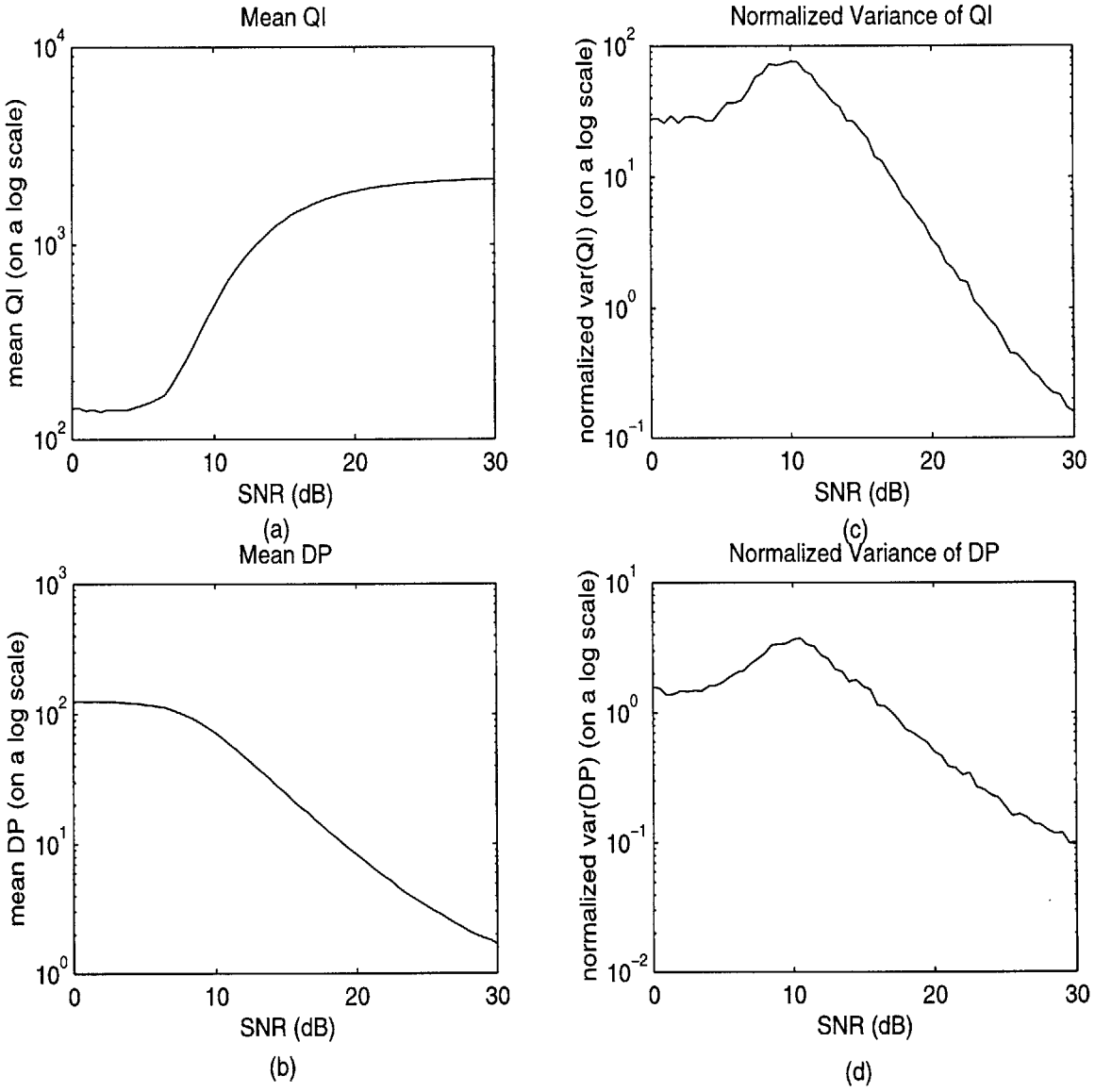

Figure 5-7: Second-order statistics of QI versus DP.

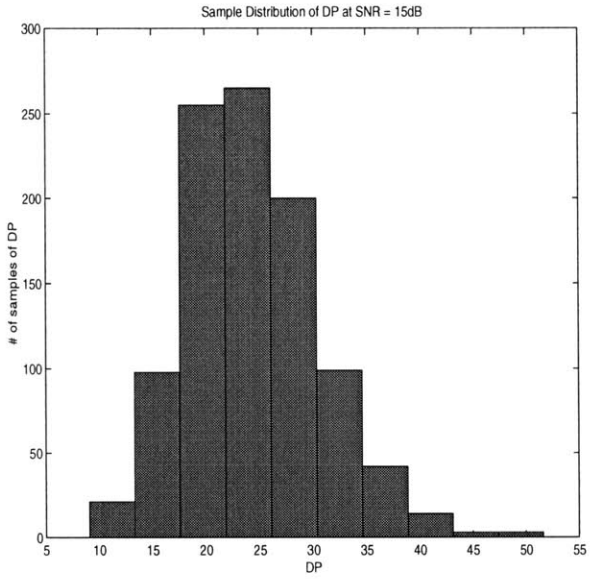

Figure 5-8: Sample Distribution of 1000 DP data points at 15dB SNR.

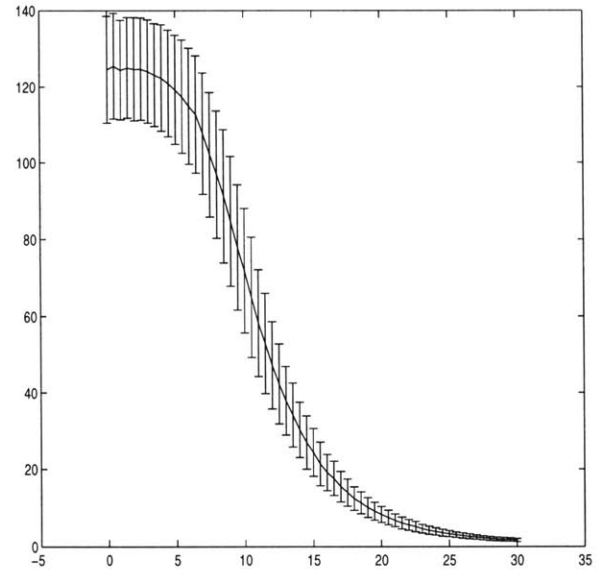

Figure 5-9: Mean QI values with Error Bars to indicate plus or minus one Standard Deviation

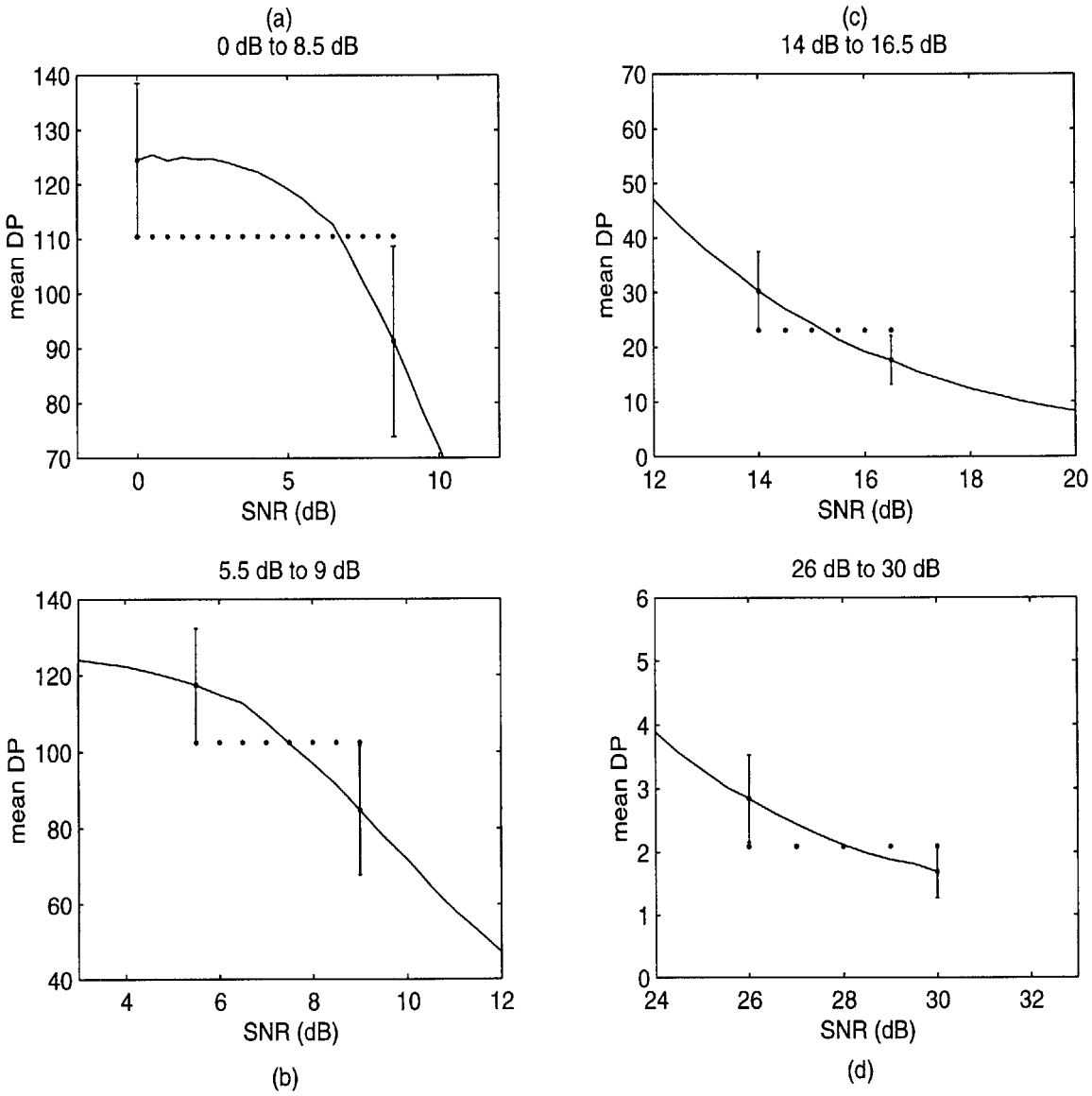

Figure 5-10: Sample Distances Between Distinguishable SNR levels for QI metric

Chapter 6

Conclusion

6.1 Summary

This thesis proposed to investigate a method of estimating the signal-to-noise ratio on a wireless channel for the purposes of performing diversity selection. It aimed to do so within the context of the PACS demodulating circuit and to take advantage of the features of the system so as to minimize the additional complexity these methods would apply. The previous chapters provide a description of the PACS system, a justification for the metrics chosen and details their relationship to noise, a description of the simulations and models used to test and verify these proposals, and a summary of the results. The method studied involved simulating the hardware, observing controlled outputs, and characterizing the statistical behavior of particular outputs. Specifically, two metrics derived from the symbol timing portion of the demodulator circuit, the QI and the DP, were proposed as two plausible candidates to be used for performing diversity selection because of the close relationship between their behavior and the noise level on the channel.

Chapter 4 describes the steps that lead up to developing a maximum likelihood estimation method for the SNR level in a channel given a particular observation of either DP or QI. We took both an analytical and a numerical approach, and the results are presented in Chapter 5. They demonstrate the correlation between the expected results derived from the analytical models to the empirical results computed from simulated data. From this, we propose that it is possible to form a maximum likelihood estimate of the noise on the channel. Through numerical methods similar to those used in this study, it is clearly possible to form an estimation scheme. In some cases, it is more difficult to confirm this analytically,

and some of these issues will be discussed in the next section when we address possible methods that can be applied but were not included within the scope of this thesis.

We also use the data to evaluate the metrics' ability to accurately discriminate between SNR levels, which returns to the ultimate purpose of performing diversity selection. Two metrics were chosen and a comparison was done in the hopes that one metric would demonstrate better performance than the other. There is some intuitive justification for presuming that DP may offer greater sensitivity than QI. QI is a representation of the projection of a unit length vector with some phase onto the real axis. Clearly, if one were to compare two QI values, if the phases of the two vectors were very close but still distinct, it may be possible, at large enough SNR values, that the projection would not be sensitive to these slight differences. DP, on the other hand, is a direct measure of the phase angle. This suggests that DP would be a better discirminator. However, the results show that, indeed, it is only slightly better, and for the most part, cannot offer any significant advantage over QI.

However, that is not to say that integrating DP into the system will not offer other advantages to QI. DP does have the disadvantage that in order to calculate it, we require its mean to be calculated by the system. This may create minor delay in the computation of the metric and raise issues in having to store a block of intermediate values. However, one advantage that came out of the analysis shows that DP is easily characterized into a known probability density, namely a gamma. It has passed goodness-of-fit testing for a gamma distribution, whereas the QI could not be fitted to any common. In that sense, a model using QI can only be numerically formed. While this is generally reliable, it is not possible to confirm it with any analytical results. The following section summarizes some future work that could be done to continue the analysis done in this study. Included in this address will be some numerical and statistical methods for evaluating the nature of QI and DP further.

6.2 Future Work

6.2.1 Possible Numerical Methods

As discussed above, an analytical model cannot be easily applied to the evaluation of QI without any first-order knowledge of its distribution. Instead, we must rely on numerical

methods and simulation if we hope to be able to form some one-to-one relationship between QI and SNR. The observed data can be collected at a given SNR level. The distribution of the data represents the probability density distribution of the QI conditioned on SNR if taken over a large number of samples.

If the distribution is unimodal, which is a characteristic we observed in Section 5.1.1, then the most likely value of QI given a particular SNR level is easily identified as the peak of the distribution. Naturally, using discrete samples to approximate a distribution requires some binning, and therefore, the peak will, in reality, be associated with a range of QI values. Taking the center of this bin as the absolute value associated with the particular SNR level naturally introduces some error into the approximation, but given small enough bins, it may have only a nominal effect. Running Monte Carlo simulation of the system at different SNR levels will result in a collection of QI values, each associated with a particular SNR. Using these tabulated results, it is then possible to match an observed QI value with its most likely associated SNR level.

6.2.2 Possible Analytical Methods

However, if a relationship between a metric and SNR can be established, as is the case with DP, and its expected behavior has been verified, further characterization of the metrics is possible. The second-order statistics discussed in Section 3.3.2 and Section 4.4 help to derive and verify the probability densities of the metrics conditioned on a given SNR level.

However, QI is the parameter actually observed and measured, and the distribution being verified is really $p(QI|SNR)$ Ultimately, some relationship must be drawn that will lead to the ability to estimate SNR levels given a QI.

Since the distribution of QI conditioned on SNR can be approximated by the data, only the a priori density of SNR needs to be assumed before the joint probability density of QI and SNR can be estimated. Once the joint pdf has been calculated, over quantized levels of SNR and QI, the density of SNR conditioned on QI is given by a simple instantiation of Bayes' Rule.

$$p_{x|y}(X|Y) = \frac{p_{x,y}(X,Y)}{p_y(Y)} \tag{6.1}$$

This line of analysis was not pursued in this study because the nature of the a priori

probabilities is difficult to characterize. However, given enough information about the design of the system and the statistical specifications of the receive, it may be possible to formulate a reasonable model of the behavior of SNR on the channel. From this, the Bayesian analysis described above would be extremely helpful in developing an exact estimation technique for SNR on the channel.

6.3 Concluding Remarks

This study aimed to develop an effective method of estimating SNR given an observation of a metric produced by the system. It was originally hoped that the QI, already in place as a symbol timing metric, might be able to offer this function. Although the analysis of QI did not yield promising results, they did provide some interesting insight into its dependence on the SNR levels of the channel, the algorithm, and the model developed to analyze its behavior. In fact, QI is clearly linked to SNR in a statistical fashion. Unfortunately, the degree of correlation is too low to establish any reliable estimation rules. The fact that QI did not prove useful in estimating SNR genuinely motivates research into alternative metrics. As a result, DP was the second metric investigated. While the analysis on this metric was much more defined and reliable, it was not able to demonstrate significantly better performance than the QI.

However, several useful analysis systems appear to be well-suited to further investigation of these metrics and others. The current diversity selection method implemented on the PACS system does not appear to be less reliable than the new one proposed in this study, and it seems to be capable of performing the discrimination required. However, even more reliable performance may be attainable. It is the hope that the methods described in this study can be easily applied to the evaluation of other metrics as well.

Appendix A

Simulation Code

```
% QIDPsim.m
%
% Parallel implementation of demodulator code for QI amd DP testing
% Symbol timing implemented one burst vector at a time.
% no carrier recovery implementation

invp1=ones([1 1200]); % bit to account for any inversions in IF
invp2=ones([1 1200]); % note using ZEROS with 10.7 MHz IF sampling!
                      % since 3*3840 - 10700 is HIGH SIDE injection
                      % but so is 960 kHz into 820 kHz actual IF

% IF compensation to add 140 kHz
% done as 9,9,10,9,9,10 brad per sample! (9,9,9,... would give
% only 135 kHz)
% deal with wraparound
ifcomp=modulo((0:1199)*140/3840*2*pi,2*pi);

stmax1=zeros([1 3]); % symbol timing results nmetric, gate val, freq offset
stmax2=zeros([1 3]);
```

```
% filter coefficients
bpfilt=[1,0,-1];
lpfilt=[1,2,2,2,1];

nburst=100;
clip=input('Clipping fraction of peak-to-peak? ');

% assume first sample in data sequence is beginning of burst;
% allow offset for tcburst timing
soff=input('Number of samples to offset tcburst timing? ');

psrc=sqrtrc((-60:60)/20,0.5); % square-root RC response
% NOTE: length 121 - for 6 extra symbols + 1 for convolution
% (for one burst)

dph=pi/4*[1 3 -1 -3]; %matrix of differential phases

foff=0;
for SNR = 0:0.5:30,

for burstcnt=1:1000,
% generate a differential phase sequence - JL 7/6/98
dphseq=dph(floor(4*rand(1,53))+1);
%generate a phase sequence
  phseq=cumsum([0, dphseq]);
phseq=modulo(phseq,pi); %%
%generate 20x oversampled baseband sequence
phseq20=[exp(j*phseq);zeros(19,54)];
bbseq=phseq20(:)';

fbbseq=conv(bbseq,psrc);
```

```
%add AWGN
%multiply variance by 20 to compensate for 20x oversampling
var=20*10^(-SNR/10);
dev=sqrt(var/2);
nI=dev*(randn(size(fbbseq)));
nQ=dev*(randn(size(fbbseq)));
nseq=nI+j*nQ; %making complex noise

fbbseq1=fbbseq+nseq;
fbbseq2=conv(fbbseq1,psrc)/20; % does sqrt RC filtering - divide by 20
fbbseq2=fbbseq2(61:length(fbbseq2)-60);
%throw away first and last 60 samples

% optional frequency offset <foff>
% now mix up to IF
% the actual IF frequency is -820 kHz (10700 - 3*3840)
ifseq1=real(exp(j*2*pi*(foff-820)/192*(0:1199)/20) .* fbbseq1);
ifseq2=real(exp(j*2*pi*(foff-820)/192*(0:1199)/20) .* fbbseq2);

% clear accumulators
stIa=zeros([1 20]);
stQa=zeros([1 20]);
stIb=zeros([1 20]);
stQb=zeros([1 20]);

% bandpass filtering and mix down from IF /
        % image reject low pass filter (throw away first 7 samples)
fifseq1=conv(ifseq1,bpfilt);
fifseq2=conv(ifseq2,bpfilt);

fifseq1=fifseq1(3:1202);
fifseq2=fifseq2(3:1202);
```

```
xout1=conv(fifseq1.*cos(pi*(0:length(fifseq1)-1)/2),lpfilt);
yout1=conv(fifseq1.*sin(pi*(0:length(fifseq1)-1)/2),lpfilt);
xout1=xout1(5:1204);
yout1=yout1(5:1204);
xout2=conv(fifseq2.*cos(pi*(0:length(fifseq2)-1)/2),lpfilt);
yout2=conv(fifseq2.*sin(pi*(0:length(fifseq2)-1)/2),lpfilt);
xout2=xout2(5:1204);
yout2=yout2(5:1204);

romout1=atan2(yout1,xout1);
romout2=atan2(yout2,xout2);

% compensate for IF offset
        % nominal 820 kHz (3*3840 kHz - 10700 kHz), but expecting 960 kHz
        ph8a=modulo(romout1-ifcomp,2*pi);
ph8b=modulo(romout2-ifcomp,2*pi);

% update input to x & y accumulation in symbol timing
% NOTE another do2scomp for case diff phase > 127 ?
% pad dph8 to 1200 samples for consistency, with 20 leading zeroes
dph8a(1:20)=zeros([1 20]);
dph8a(21:1200)=ph8a(21:1200)-ph8a(1:1180);

dph8b(1:20)=zeros([1 20]);
dph8b(21:1200)=ph8b(21:1200)-ph8b(1:1180);


%%%%% calculations for QI %%%%%

% simulate sin4theta and cos4theta lookup ROMs
c4a=cos(4*dph8a); % cos4theta lookup picks vals at address VECTOR indices
```

```
s4a=sin(4*dph8a); % sin4theta lookup picks vals at address VECTOR indices

c4b=cos(4*dph8b); % cos4theta lookup picks vals at address VECTOR indices
s4b=sin(4*dph8b); % sin4theta lookup picks vals at address VECTOR indices


%%%%% calculations for DPe %%%%%

dph4a=modulo(4*dph8a,2*pi)-pi;
dph4b=modulo(4*dph8b,2*pi)-pi;

% 14 bit signed accumulation (-8192 to +8191)
% use zerov to accum middle of burst
% 6 symbols LOW; 47 symbols HIGH; 7 symbols LOW - JL 7/6/98
start=120+soff;
finish=1060+soff;
% this is right - sum up every 20 samples over a block of 20
for zzz=1:20,
stIa(zzz)=sum(c4a((zzz+start):20:finish));
stQa(zzz)=sum(s4a((zzz+start):20:finish));
stIb(zzz)=sum(c4b((zzz+start):20:finish));
stQb(zzz)=sum(s4b((zzz+start):20:finish));
norma(zzz)=norm(dph4a((zzz+start):20:finish))^2;
normb(zzz)=norm(dph4b((zzz+start):20:finish))^2;
end

nmetric1=stIa.^2+stQa.^2;
nmetric2=stIb.^2+stQb.^2;

dpmetricsa(SNR*2000+burstcnt)=min(norma);
dpmetricsb(SNR*2000+burstcnt)=min(normb);
```

```
qimetricsa(SNR*2000+burstcnt)=max(nmetric1);
qimetricsb(SNR*2000+burstcnt)=max(nmetric2);

end
end
```

References

[1] Siavash M. Alamouti, "A Simple Transmit Diversity Technique for Wireless Communications" in *IEEE Journal on Selected Areas in Communications*, October 1998, pp. 1451-1458.

[2] "PACS Providers Forum," *http://www.pacs.org.*

[3] J. C-I Chuang and N.R. Sollenberger, "Burst Coherent Demodulation with Combined Symbol Timing, Frequency Offset Estimation and Diversity Selection," *IEEE Trans. On Comm.*, vol. 39, no. 7, pp. 1157-1164, July, 1991.

[4] N. R. Sollenberger, J. C-I Chuang, "Low-Overhead Symbol Timing and Carrier Recovery for TDMA Portable Radio Systems," *IEEE Trans. on Comm.*, October, 1990, pp. 1886-1892.

[5] C. L. Liu and K. Feher, "A new generation of Rayleigh fade compensated pi/4-QPSK coherent modem", *Proc. 40th IEEE Veh. Conf., Orlando, FL,* May 1990, pp. 482-486.

[6] W. T. Webb and L. Hanzo, *Modern Quadrature Amplitude Modulation.* London: Pentech Press, 1994, pp. 98-114.

[7] N.R. Sollenberger, "An Experimental VLSI Implementation of Low-Overhead Symbol Timing and Frequency Offset Estimation for TDMA Portable Radio Applications," *IEEE GLOBECOM '90,* San Diego, CA, December 2-5, 1990, pp. 1701-1711.

[8] S. Ariyavisitakul, H. Arnold, L.F. Chang, J. C-I Chuang, N.R. Sollenberger, "Architecture and Implementation of Efficient and Robust TDMA Frame Structure for Digital Portable Communications," *IEEE Trans. On Veh. Tech.*, vol. 40, pp. 250-260, Feb. 1991.

[9] Paul L. Meyer, *Introductory Probability and Statistical Application.* Reading, Massachusetts: Addison-Wesley, 1970, pp. 328-335.